Quantum Electronics **31** (7) 569 – 586 (2001)

REVIEW

PACS numbers: 32.50.+d; 78.67.–n
DOI: 10.1070/QE2001v031n07ABEH002007

Spontaneous emission of an atom in the presence of nanobodies

V V Klimov, M Ducloy, V S Letokhov

Contents

Contents

Abstract. **The effect of nanobodies, i.e., the bodies whose size is small compared to the emission wavelength, on spontaneous emission of an atom located near them is considered. The results of calculations performed within the framework of quantum and classical electrodynamics are presented both in analytic and graphical forms and can be readily used for planning experiments and analysis of experimental data. It is shown that nanobodies can be used to control efficiently the rate of spontaneous transitions. Thus, an excited atom located near a nanocylinder or a nanospheroid pole, whose transition dipole moment is directed normally to the nanobody surface, can decay with the rate that is tens and hundreds times higher than the decay rate in a free space. In the case of some (negative) dielectric constants, the decay rate can increase by a factor of $10^5 - 10^6$ and more. On the other hand, the decay of an excited atom whose transition dipole moment is directed tangentially to the nanobody surface substantially slows down. The probability of nonradiative decay of the excited state is shown to increase substantially in the presence of nanobodies possessing losses.**

Keywords: *atoms, spontaneous emission, nanobodies.*

V V Klimov P N Lebedev Physics Institute, Russian Academy of Sciences, Leninskii prosp. 53, 119991 Moscow, Russia
M Ducloy Laboratoire de Physique des Lasers, UMR CNRS 7538 University Paris-Nord, Institut Galilee, Avenue J-B. Clement-F93430, Villetaneuse, France
V S Letokhov Institute of Spectroscopy, Russian Academy of Sciences, 142092 Troitsk, Moscow oblast, Russia

Received 19 January 2001
Kvantovaya Elektronika **31** (7) 569 – 586 (2001)
Translated by M N Sapozhnikov

1. Introduction

Since our review, as follows from its title, seems to be more concerned with atomic physics than with quantum electronics, it is reasonable to begin with an extended introduction using the terms accepted in quantum electronics.

An excited quantum system can emit light spontaneously and in a stimulated way, as has been predicted by Einstein in his theory of equilibrium emission [1] and has been rigorously shown by Dirac in the quantum theory of emission [2]. According to the Dirac theory, the probability of the photon emission to a given mode (field oscillator, etc.) is proportional to $1 + N$, where the first term corresponds to spontaneous emission and the second term corresponds to stimulated emission (N is the number of photons in the oscillation mode under study). The total probability of spontaneous decay of the excited state 2 of a quantum system to the lower state 1 is determined by the Fermi golden rule [3]

$$\gamma_{21} \sim |d_{21}|^2 \rho_{21}(\omega), \tag{1}$$

where d_{21} is the matrix element coupling states 2 and 1; $\rho_{21}(\omega)$ is the density of modes of electromagnetic oscil-

lations at the transition frequency ω. In a free space, $\rho(\omega)$ is described by the known Rayleigh – Jeans formula, i.e., it depends only on the frequency ω and the quantisation volume.

A resonator system separates a limited number of high-Q oscillation modes, in which spontaneous quanta are multiplied due to stimulated transitions in an *amplifying medium* inside the resonator. Therein lies, as is known, the fundamental principle of masers and lasers [4, 5]. In a maser, this effect is achieved with the help of a *closed* (volume) resonator of volume $V \sim \lambda^3$ (λ is the emission wavelength), which *simultaneously* restricts the number of oscillation modes both for spontaneous and stimulated emission. In a laser, this effect is achieved using an *open* resonator of volume $V \gg \lambda^3$ [6, 7], which separates a limited number of high-Q oscillation modes of stimulated emission, which develops from a very weak spontaneous emission into these separated oscillation modes. At the same time, a huge number of the rest of the modes can be involved in spontaneous emission virtually without any restrictions.

In a good laser operating well above the threshold, the total probability of stimulated emission of an atom to a small number of high-Q oscillation modes is much greater than the total probability of spontaneous emission of the atom to a very great number of the rest of the oscillation modes. For this reason, in most cases a relatively weak spontaneous emission does not strongly affect the fundamental characteristics of laser radiation, whereas a very weak spontaneous emission into high-Q oscillation modes of the laser plays an important role in the phase fluctuations of the coherent field of the laser, i.e., in the establishment of the limiting spectral width of a laser line [7]. Until recently, quantum electronics has been successfully developed by using controllable stimulated quantum processes for improving all the parameters of laser radiation, whereas the question of controlling an elementary process of spontaneous emission remained open.

However, the problem of controlling the quantum process of spontaneous emission is no less important from the general point of view than the control of stimulated emission. Suffice it to say that we use the artificial illumination that is mainly produced by the transformation of electricity to spontaneous light and the control of this process is far from perfect. Only recently, due to the development of heterostructure light emitting diodes [8], we have approached to the creation of highly efficient electric sources of bright spontaneous emission at the required wavelength, which will have a great practical consequence in the future. However, now of interest to us is the question of controlling an elementary event of spontaneous emission of light.

This question has been formulated for the first time by Purcell [9] who considered the enhancement of the probability of spontaneous emission for an atom in a resonator whose the only oscillation mode frequency was tuned to the transition frequency of the atom. The spontaneous emission rate A_c in the resonator can achieve the value $\sim AQ$, where A is the spontaneous emission rate for the atom in a free space and Q is the quality factor of the resonator. In Ref. [10], the theory of spontaneous emission of an atom in a resonator has been developed, which is valid for any detuning of the oscillation mode frequency of the resonator with respect to the quantum transition frequency in the atom. It is clear within the framework of these concepts that the spontaneous decay rate of the atom decreases when the resonator frequency and the quantum transition frequency in the atom are detuned, and if the fundamental frequency of the quantum transition is lower than the frequency of the fundamental (lowest) resonator mode, spontaneous emission can be substantially inhibited [11].

The increase in the spontaneous emission rate has been observed for the first time at the transitions between highly excited (Rydberg) states of an atom in a submillimetre range when the atom flied through a miniature high-Q resonator [12]. Then, the inhibition of spontaneous emission was observed. Thus, in paper [13], the 20-fold inhibition was observed at Rydberg transitions, while in paper [14] this effect was observed for cyclotron emission of one electron in the Penning trap used as a resonator. By omitting the subsequent theoretical and experimental papers, note that all this scope of problems is described by the so-called cavity quantum electrodynamics (CQED) [15, 16].

After the first experiments in the microwaves region, the inhibition of spontaneous emission in the optical range was observed [17], and now it seems that this field of CQED will be developed in succeeding years. This is related both to the advances in the laser technologies and to the development of new micro- and nanostructured optical materials, Here, we can distinguish three fields of investigations.

(1) The development of microlasers with the cavity volume V comparable with λ^3. In this case, the number of oscillation modes becomes small even within a broad gain line, i.e., the situation appears that is similar to the laser limit. The number of oscillation modes decreases both for spontaneous and stimulated transitions. By controlling the density and positions of resonances, one can control both spontaneous and stimulated emission. This scope of problems involves experiments with microspheres, which have high Q factors in the optical range [18 – 20] (they have been already used in microlasers with ultralow lasing threshold [21, 22]), microdroplets of the amplifying medium [23, 24], planar microcavities (vertical cavity surface emitting lasers (VCSEL) [25, 26]), photonic quantum wires [27], photonic quantum dots [28], etc.

(2) The fabrication of three-dimensional periodic dielectric structures of size $L \gg \lambda$, but with the period of variation in, for example, the refractive index of the order of λ. In such structures, which are now called photonic crystals, spontaneous emission can be substantially inhibited [29 – 33]. However, the field of application of photonic crystals [34, 35] is not restricted only by controlling spontaneous emission of their atoms because these crystals substantially change the properties of the light propagation. Suffice it to recall a simplest one-dimensional quasi-periodic structure, an interference filter.

(3) The variation of boundary conditions, which also affect the properties of spontaneous emission. This follows from the first observation of a decrease in the fluorescence emission rate for polyatomic dye molecules near a metal or dielectric surface [36, 37]. This effect has a nonresonance nature because it is caused by the interaction of a dipole with its mirror image. The boundary conditions distort the spectrum of modes into which the atom can emit spontaneously, resulting in a change in the spontaneous emission rate. This effect can be especially substantial near nanostructures, which distort the field distribution at distances that are smaller than the emission wavelength or comparable to it. It is this field of studies – the spontaneous emission of an atom near nanobodies of various shapes – that is the topic of our review.

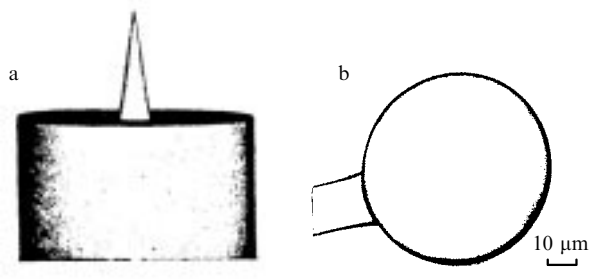

Figure 1. Examples of nanobodies: the tip of a scanning microscope (the radius of curvature of the tip end is ~ 1 nm) photographed using a tunnel electron microscope (see [38], pp. 131–139) (a) and microsphere photographed using a tunnel electron microscope [20] (b)

Modern technologies make it possible to create various objects and structures with characteristic sizes as small as hundreds and even tens of nanometres. The tips of aperture and apertureless scanning microscopes belong first of all to such structures [38–47]. Fig. 1a shows a typical nanobody - a tip of a scanning microscope. Here, a thick cylinder is a usual fibre of diameter ~ 1.6 μm on which a tip is etched with a characteristic size near the end of about 1 nm. Such tips are used in various scanning microscopes.

At present, the so-called apertureless scanning microscopes [42–45], in which a sample is illuminated by a broad light beam and the light scattered by the sample upon approaching the tip to it is detected, are considered the most promising. An apertureless microscope of another type was proposed in paper [46]. In this microscope, a submicron active medium replaces the aperture and acts as a localised light source. Moreover, in papers [46, 47] the schemes were proposed in which an active medium (a light source) was a single molecule. Such schemes can be efficiently used for surface imaging with a high spatial (better than 1 nm) and high spectral resolution. In addition, Raman scattering substantially enhances near the tip [48, 49], which allows one to analyse the chemical composition of the sample.

Another interesting case of the effect of nanoobjects on emission is colloidal solutions of nanoparticles of different shape. In particular, it was shown in paper [50] that the solution of gold microspheres of diameter 35 nm does not emit fluorescence, whereas fluorescence is enhanced by 6–7 orders of magnitude in the solution of gold nanorods of the same volume.

Other microobjects being actively studied are dielectric micro- and nanospheres (Fig. 1b), which have high Q factors in the optical range [18–20]. Such microspheres have been already used for manufacturing microlasers with the ultralow lasing threshold [21, 22]. In paper [51], the technologies of fabrication of layered nanospheres with a broad range of resonance properties have been described.

Note the principal difference between microspheres and nanospheres. The size of nanospheres is less than the wavelength of light and their action is mainly caused by large field gradients near them. In microspheres, optical resonances can be excited (whispering gallery modes), resulting in a strong resonance interaction with atomic transitions. The case of microspheres is very interesting but lies beyond the scope of this review.

The cylindrical geometry is also quite important in applications of nanotechnologies. Thus, the authors of papers [52, 53] measured fluorescence of single molecules in submicron capillaries. On the other hand, the effect of submicron conductors on spontaneous emission can be important for the confinement of atoms with the help of charged conductors [54, 55].

An important property of nanobodies is their ability to change substantially the rates of forbidden transitions. In papers [56, 57], a strong increase in the rate of electric quadrupole transitions near a sphere and a cylinder of small sizes was demonstrated. The authors of paper [58] proposed to use a dielectric fibre for the experimental study of forbidden transitions in atoms flying near the fibre.

Thus, in many practically important cases it is necessary to know the effect of nanoobjects on atoms. In particular, of great interest is the problem of fluorescence of atoms near nanoobjects, i.e., the effect of nanobodies on the spontaneous decay rates in atoms. In this review, which is mainly based on our studies, we consider briefly the features of spontaneous emission near nanobodies of various shapes. We assume that nanoobjects consist of nonmagnetic materials without dispersion.

Note that the problems under study belong to a new field of research – nanooptics, which in turn represents a part of nanotechonolgy – one of the key technologies of the XXI century.

2. Elements of the theory of spontaneous emission of an atom in the presence of material bodies

2.1 Classical approach: radiative back reaction on an oscillator

Within the framework of the classical approach [16, 59], an atom can be modelled by a classical oscillator consisting of a charge $-e$ at rest located at the point $\boldsymbol{r}'$ and of a charge e located at the point $\boldsymbol{r} = \boldsymbol{r}' + \delta\boldsymbol{r}$ and oscillating around the first charge. The equation of motion of the oscillating charge in a free space has the form

$$m\delta\ddot{\boldsymbol{r}} + m\gamma_0\delta\dot{\boldsymbol{r}} + m\omega_0^2\delta\boldsymbol{r} = 0. \tag{2.1}$$

Here, $\delta\boldsymbol{r}$ is the displacement of the oscillating charge from the equilibrium position;

$$\gamma_0 = \frac{2e^2}{3c^3}\frac{\omega_0^2}{m} \tag{2.2}$$

is the spontaneous decay rate in vacuum; m is the mass of the oscillating charge; and ω_0 is the oscillation frequency in vacuum.

The oscillator located at the point $\boldsymbol{r}'$ near some body is subjected to the additional (compared to the oscillator in a free space) field $\boldsymbol{E}^{(1)}(\boldsymbol{r}')$, so that the equation of motion takes the form

$$\begin{aligned} m\ddot{\boldsymbol{d}} + m\gamma_0\dot{\boldsymbol{d}} + m\omega_0^2\boldsymbol{d} &= e^2\boldsymbol{E}^{(1)}(\boldsymbol{r}' + \delta\boldsymbol{r}, t) \\ &\approx e^2\boldsymbol{E}^{(1)}(\boldsymbol{r}', t), \end{aligned} \tag{2.3}$$

where $\boldsymbol{d} = e\delta\boldsymbol{r}$ the electric dipole moment of the oscillator. To find the reflected field $\boldsymbol{E}^{(1)}(\boldsymbol{r}')$, one should solve a complete system of Maxwell's equations, in which a source of the charge and current is the dipole moment of the oscillator

$$\rho = -(\boldsymbol{d}_0\nabla)\delta(\boldsymbol{r}-\boldsymbol{r}')\mathrm{e}^{-\mathrm{i}\omega t},\ \boldsymbol{j} = -\mathrm{i}\omega\boldsymbol{d}_0\delta(\boldsymbol{r}-\boldsymbol{r}')\mathrm{e}^{-\mathrm{i}\omega t}. \quad (2.4)$$

Assuming that all the quantities are proportional to $\exp(-\mathrm{i}\omega t)$, we can obtain from (2.3) the dispersion equation for determining the parameters of the atomic oscillator in the presence of an arbitrary body:

$$\omega^2 + \mathrm{i}\omega\gamma_0 - \omega_0^2 + \frac{e^2}{md_0^2}\boldsymbol{d}_0\boldsymbol{E}^{(1)}(\boldsymbol{r}',\omega) = 0, \quad (2.5)$$

where $\boldsymbol{d}_0$ is the amplitude of the dipole oscillations.

In the small-correction approximation, the solution of (2.5) can be written in the form

$$\omega = \omega_0 - \frac{\mathrm{i}}{2}\gamma_0 - \frac{e^2}{2m\omega_0}\frac{\boldsymbol{d}_0\boldsymbol{E}^{(1)}(\boldsymbol{r}',\omega_0)}{d_0^2}. \quad (2.6)$$

By separating the real and imaginary parts in (2.6) and using expression (2.3) for the transition rate in vacuum, we obtain in this approximation the expression for the change in the spontaneous decay rate [59]

$$\frac{\gamma}{\gamma_0} = 1 + \frac{3}{2}\mathrm{Im}\,\frac{\boldsymbol{d}_0\boldsymbol{E}^{(1)}(\boldsymbol{r}',\omega_0)}{d_0^2k_0^3}, \quad (2.7)$$

where $k_0 = \omega_0/c$ and $k = \omega/c$ are the wave numbers in a free space. Note that expression (2.7) is also valid in the case of a complex dielectric constant, i.e., for a substance with losses.

2.2 Classical approach: the energy flux at infinity

The spontaneous decay rate in the absence of losses in a substance can be also found directly, by calculating the intensity of emission for the atom + body system at infinity and dividing this energy flux to the energy flux from the oscillator in a free space:

$$\frac{\gamma}{\gamma_0} = \frac{\int\left|\left[\left(\boldsymbol{E}^{(0)}+\boldsymbol{E}^{(1)}\right)\left(\boldsymbol{H}^{(0)}+\boldsymbol{H}^{(1)}\right)\right]_{r\to\infty}\right|^2\mathrm{d}\Omega}{\int\left|\left[\boldsymbol{E}^{(0)}\boldsymbol{H}^{(0)}\right]_{r\to\infty}\right|^2\mathrm{d}\Omega}. \quad (2.8)$$

Here, the integration is performed over the solid angle $\mathrm{d}\Omega$. In the case of nanoobjects of interest to us, we deal with dipole emission and expression (2.8) is reduced to the ratio of squares of dipole moments

$$\frac{\gamma}{\gamma_0} = \frac{|\boldsymbol{d}_{\mathrm{tot}}|^2}{|\boldsymbol{d}_0|^2}, \quad (2.9)$$

where $\boldsymbol{d}_{\mathrm{tot}}$ is a total dipole moment of the atom + nanobody system.

Therefore, to find the change in the spontaneous decay rate in the presence of any nanoobject whose size is small compared to the emission wavelength, it is sufficient to solve a quasi-static problem for a dipole near this object. In this case, a total dipole moment, according to Eqn (2.9), allows us to find the change in the spontaneous decay rate.

In principle, we can use expression (2.7) for calculating the change in the spontaneous decay rate near nanoobjects. However, in this case we should solve either a complete electrodynamic problem (which is often impossible to do analytically) or several static problems to construct the perturbation theory in the wave vector $\boldsymbol{k}$ [60]. Note that expressions (2.8) and (2.9) are based on the calculation of the emission flux at infinity and, hence, they cannot be applied to substances with losses inside which the energy flux is present.

2.3 Quantum-mechanical approach

The quantisation procedure of an electromagnetic field in the presence of dielectrics without losses is known as a whole [61]. However, a special approach is required in each specific case. In the problem of the spontaneous decay, it is convenient to consider standing waves as a basis. For this purpose, the atom + nanobody system should be placed inside the quantisation volume of a large size ($\Lambda \to \infty$). The geometry of the quantisation volume is determined by the geometry of the problem, and the volume size does not enter to observables. The expansion of the quantised electromagnetic field and its vector potential over the full system of eigenfunctions of the classical problem (over standing waves) can be written in the form

$$\hat{\boldsymbol{E}} = \sum_{\boldsymbol{s}}\frac{a_{\boldsymbol{s}}\boldsymbol{e}(\boldsymbol{s},\boldsymbol{r}) - a_{\boldsymbol{s}}^{+}\boldsymbol{e}^{*}(\boldsymbol{s},\boldsymbol{r})}{\mathrm{i}\sqrt{2}},$$

$$\hat{\boldsymbol{B}} = \sum_{\boldsymbol{s}}\frac{a_{\boldsymbol{s}}\boldsymbol{b}(\boldsymbol{s},\boldsymbol{r}) + a_{\boldsymbol{s}}^{+}\boldsymbol{b}^{*}(\boldsymbol{s},\boldsymbol{r})}{\sqrt{2}}, \quad (2.10)$$

$$\hat{\boldsymbol{A}} = -\sum_{\boldsymbol{s}}\frac{c}{\omega_{\boldsymbol{s}}}\frac{a_{\boldsymbol{s}}\boldsymbol{e}(\boldsymbol{s},\boldsymbol{r}) + a_{\boldsymbol{s}}^{+}\boldsymbol{e}^{*}(\boldsymbol{s},\boldsymbol{r})}{\sqrt{2}}.$$

Here, $a_{\boldsymbol{s}}$, $a_{\boldsymbol{s}}^{+}$ are the annihilation and creation operators of photons for the corresponding modes, which satisfy the usual commutation relations; and $\omega_{\boldsymbol{s}}$ are frequencies of these modes. The subscript $\boldsymbol{s}$ is a composite one (vector) and includes the mode type (TE or TM) and quantum numbers, which are similar to the quantum numbers of a one-electron atom.

Maxwell's equations, which determine the modes, have the form

$$\nabla\times\boldsymbol{e}(\boldsymbol{s},\boldsymbol{r}) = \frac{\omega_{\boldsymbol{s}}}{c}\boldsymbol{b}(\boldsymbol{s},\boldsymbol{r}),,$$
$$\nabla\times\boldsymbol{b}(\boldsymbol{s},\boldsymbol{r}) = -\frac{\omega_{\boldsymbol{s}}}{c}\varepsilon(\boldsymbol{r})\boldsymbol{e}(\boldsymbol{s},\boldsymbol{r}) \quad (2.11)$$

where $\varepsilon(\boldsymbol{r})$ is a function describing the spatial distribution of the dielectric constant. We also assume that the wave functions of photons are normalised per photon in the quantisation volume:

$$\frac{1}{4\pi}\int\mathrm{d}^3\boldsymbol{r}\boldsymbol{e}^{*}(\boldsymbol{s},\boldsymbol{r})\boldsymbol{e}(\boldsymbol{s}',\boldsymbol{r}) = \delta_{\boldsymbol{s}\boldsymbol{s}'}\hbar\omega_{\boldsymbol{s}},$$

$$\frac{1}{4\pi}\int\mathrm{d}^3\boldsymbol{r}\boldsymbol{b}^{*}(\boldsymbol{s},\boldsymbol{r})\boldsymbol{b}(\boldsymbol{s}',\boldsymbol{r}) = \delta_{\boldsymbol{s}\boldsymbol{s}'}\hbar\omega_{\boldsymbol{s}}. \quad (2.12)$$

The interaction Hamiltonian of the quantised field with an atom can be constructed in a usual way [16]. In the case of dipole transitions, it is sufficient to retain only the first term in the full Hamiltonian:

$$H_{\mathrm{int}} = -\frac{e}{mc}\hat{\boldsymbol{A}}(\boldsymbol{r})\hat{\boldsymbol{p}} + \ldots. \quad (2.13)$$

Here, $\hat{\boldsymbol{A}}(\boldsymbol{r})$ is the vector potential operator at the electron location; $\hat{\boldsymbol{p}}$ is the electron momentum operator; and m is the electron mass.

Now, in accordance with the Fermi golden rule, the expression for the spontaneous decay rate has the form [3]

$$\gamma = \frac{2\pi}{\hbar}|\langle \mathrm{ini}|H_{\mathrm{int}}|\mathrm{fin}\rangle|^2\rho(\omega), \tag{2.14}$$

where $\rho(\omega)$ is the density of final states, which can be readily found if the solutions of Maxwell's equations are known, i.e., the spectrum of the problem.

In the case of electric dipole transitions of the E_1 type, we obtain the following expression for the spontaneous decay rate:

$$\gamma = \frac{\pi}{\hbar}|\boldsymbol{d}\boldsymbol{e}_{\mathrm{fin}}(\boldsymbol{s}, \boldsymbol{r}_0)|^2\rho(\omega), \tag{2.15}$$

where $\boldsymbol{e}_{\mathrm{fin}}(\boldsymbol{s}, \boldsymbol{r}_0)$ is the wave function of a photon in the final state and $\boldsymbol{d}$ is the matrix element of the dipole moment.

It can be shown [62] that in the absence of losses, both classical and quantum-mechanical approaches yield the same expressions for the relative transition rates, i.e., the transition rates normalised to the transition rates in a free space. For this reason, we can use any expression for calculating the spontaneous decay rate. In the case of nanobodies without internal losses, as a rule, the quantum-mechanical approach yields the result more rapidly. This is explained by the fact that in both classical approaches one should first calculate the exact Green function of a dipole source in the presence of a body and then find its asymptotic form either in the dipole vicinity ($\boldsymbol{r} \to \boldsymbol{r}'$) or at infinity ($r \to \infty$). In the case of the quantum-mechanical approach, the result is immediately expressed in the form of a relatively simple expansion over the solutions of homogeneous Maxwell's equations (2.15).

2.4 Absorbing and dispersion media

Expression (2.7) for the decay rate of a classical oscillator is valid for any (including complex) dielectric constant of the nanobody material. However, strictly speaking, quantum-mechanical expression (2.15) can be derived only by assuming that the Hamiltonian is Hermitian, i.e., in the absence of losses in the material.

In this case, the proof of the equivalence of classical and quantum-mechanical results is also valid. However, papers [63–65] were recently published in which the procedure of quantisation of electromagnetic fields was generalised to the case of dispersion and absorbing media. Within the framework of this generalised theory, the quantum-mechanical and classical calculations of spontaneous transition rates are also identical in the first order of the perturbation theory.

2.5 Experimental verification of the theory

Although the theoretical approaches discussed above are based on the fundamental principles of quantum and classical electrodynamics, the experimental verification of specific theoretical results is desirable because the concept of the dielectric constant becomes inapplicable sooner or later.

Experiments with single atoms located near macroscopic bodies are very complicated, and at present only the lifetimes of atoms and ions located near a partially reflecting flat surface have been reliably measured [36, 66]. The geometry of such experiments is shown in Fig. 2. In these experiments, fluorescence was studied in samples with different widths of a dielectric layer separating an atom or an ion from a mirror.

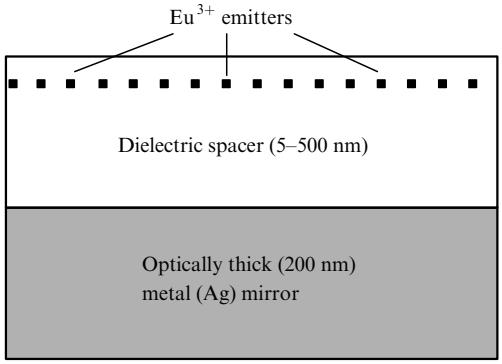

Figure 2. Geometry of the experimental setup for measurements of fluorescence of an atom located near a partially reflecting boundary.

The emission of an atom in such geometry has been well studied theoretically using both classical [59, 66] and quantum-mechanical [67] approaches. In particular, the change in the spontaneous decay rate in an atom with the perpendicular orientation of the dipole moment located at a distance z from the surface of a half-space with the dielectric constant ε is [67]

$$\begin{aligned}
\frac{\gamma}{\gamma_0} &= 1 + 3\left\{\int_0^1 \mathrm{d}t T(t)\cos(2z\omega t)\right. \\
&\quad \left. + \int_0^1 \mathrm{d}t A(t)\exp\left[-2z\omega t(\varepsilon-1)^{1/2}\right]\right\}, \\
T(t) &= \frac{1}{2}(1-t^2)\frac{\varepsilon t - (\varepsilon - 1 + t^2)^{1/2}}{\varepsilon t + (\varepsilon - 1 + t^2)^{1/2}}, \\
A(t) &= \varepsilon(\varepsilon-1)^{1/2}\frac{(\varepsilon-1)t^2+1}{(\varepsilon^2-1)t^2+1}t(1-t^2).
\end{aligned} \tag{2.16}$$

For a multilayer medium, which describes the experimental geometry more adequately, similar, but more cumbersome, expressions take place [59].

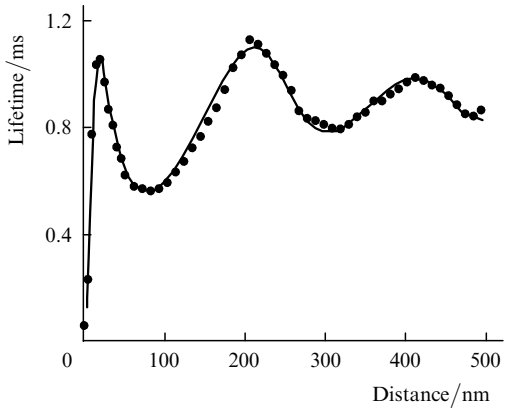

Figure 3. Experimental (circles) and calculated (solid curve) lifetimes of the excited Eu^{3+} ion located near an Ag mirror as functions of the distance to the mirror [36].

Fig. 3 shows that the measured lifetimes of the Eu^{3+} ion located near an optically thick silver mirror well agree with the corresponding theoretical curve [36] down to the distance to the mirror equal to several nanometres. This agreement demonstrates the correctness of the theoretical approaches and allows one to study theoretically (and then experimentally) spontaneous emission of an atom located near spheres, cylinders, spheroids, and cones.

The authors of paper [68] studied very recently the effect of a hole of diameter 80 nm in the aperture of a scanning microscope on spontaneous emission of a single molecule. In this paper, good agreement was obtained between experimental data and the predictions of a simple two-dimensional model when the molecular dipole moment was directed perpendicular to the aperture. In the case of other dipole-moment orientations, no agreement was observed, which means that a more exact three-dimensional model should be developed.

3. Spontaneous emission of an atom located near a dielectric microsphere

The spherical geometry has been studied most thoroughly [69–90], as a rule, using the classical approach. In our opinion, the quantum-mechanical approach in more appropriate in the spherical case whose geometry is shown in Fig. 4. The quantisation of an electromagnetic field for such geometry is also well known [83–85].

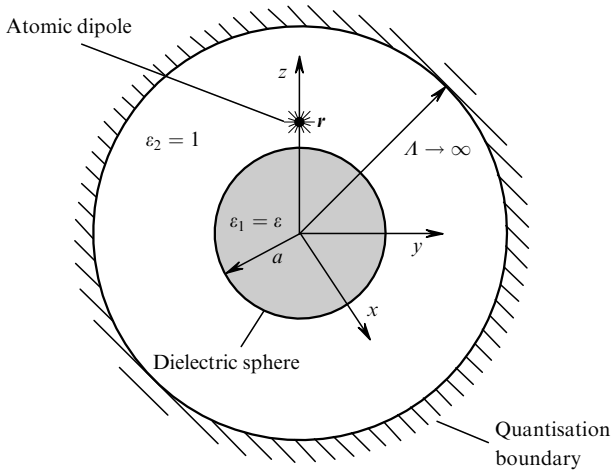

Figure 4. Geometry in a spherical case.

In the case of electric dipole transitions, both transverse magnetic (TM) and transverse electric (TE) modes can be excited. In the case of radial orientation of the transition dipole moment, only TM modes can be excited. The expressions for the electric field strength $\boldsymbol{e}(\boldsymbol{s}, r)$ of the sth mode can be readily obtained in terms of spherical harmonics Y_{nm} and spherical Hankel (h_n) and Bessel (j_n) functions [86–88]:

$$\boldsymbol{e}_{\mathrm{TM}}(n,m,\varkappa) = -\frac{1}{k_0\varepsilon_2}\nabla\times\left\{\left[\alpha^{(1)}_{\mathrm{TM}n}h^{(1)}_n(k_2r) + \alpha^{(2)}_{\mathrm{TM}n}h^{(2)}_n(k_2r)\right]\hat{\boldsymbol{L}}Y_{nm}(\vartheta,\varphi)\right\},\ r>a \tag{3.1}$$

for transverse magnetic modes and

$$\boldsymbol{e}_{\mathrm{TE}}(n,m,\varkappa) = \left[\alpha^{(1)}_{\mathrm{TE}n}h^{(1)}_n(k_2r) + \alpha^{(2)}_{\mathrm{TE}n}h^{(2)}_n(k_2r)\right]\hat{\boldsymbol{L}}Y_{nm}(\vartheta,\varphi),\ r>a \tag{3.2}$$

for transverse electric modes. Here, m, n, and $\varkappa$ are the azimuthal, orbital, and radial quantum numbers; $k_{1,2}=\varepsilon_{1,2}^{1/2}k = \varepsilon_{1,2}^{1/2}\omega(n,\varkappa)/c$ are the wave numbers inside the sphere and outside it; $k=\omega/c$ is the wave number in a free space; $\hat{\boldsymbol{L}} = -\mathrm{i}[\boldsymbol{r}\nabla]$ is the angular momentum operator; and a is the microsphere radius. The set of quantum numbers $n, m, \varkappa$ forms the vector index $\boldsymbol{s}=\{n,m,\varkappa\}$ used above. Similar expressions are valid for the electric field inside a sphere and for magnetic fields.

The coefficients $\alpha^{(1,2)}_{\mathrm{TM}n,\mathrm{TE}n}$ can be found in a usual way from the condition of the continuity of the tangential components of the field at the sphere boundary and the normalisation of the wave functions in a sphere of radius Λ per one photon in the quantised mode:

$$\frac{\alpha^{(1)}_{\mathrm{TM}n}}{\alpha^{(2)}_{\mathrm{TM}n}} = 1-2q_n, \tag{3.3}$$

$$q_n = \left\{\varepsilon_1\frac{\mathrm{d}}{\mathrm{d}z_2}[z_2j_n(z_2)]j_n(z_1) - \varepsilon_2\frac{\mathrm{d}}{\mathrm{d}z_1}[z_1j_n(z_1)]j_n(z_2)\right\} \times\left\{\varepsilon_1\frac{\mathrm{d}}{\mathrm{d}z_2}\left[z_2h^{(1)}_n(z_2)\right]j_n(z_1) - \varepsilon_2\frac{\mathrm{d}}{\mathrm{d}z_1}[z_1j_n(z_1)]h^{(1)}_n(z_2)\right\}^{-1},$$

$$\frac{\alpha^{(1)}_{\mathrm{TE}n}}{\alpha^{(2)}_{\mathrm{TE}n}} = 1-2p_n, \tag{3.4}$$

$$p_n = \left\{\frac{\mathrm{d}}{\mathrm{d}z_2}[z_2j_n(z_2)]j_n(z_1) - \frac{\mathrm{d}}{\mathrm{d}z_1}[z_1j_n(z_1)]j_n(z_2)\right\} \times\left\{\frac{\mathrm{d}}{\mathrm{d}z_2}\left[z_2h^{(1)}_n(z_2)\right]j_n(z_1) - \frac{\mathrm{d}}{\mathrm{d}z_1}[z_1j_n(z_1)]h^{(1)}_n(z_2)\right\}^{-1},$$

$$\left|\alpha^{(1)}_{\mathrm{TM}n}\right|^2 = \left|\alpha^{(2)}_{\mathrm{TM}n}\right|^2 = \left|\alpha^{(1)}_{\mathrm{TE}n}\right|^2 = \left|\alpha^{(2)}_{\mathrm{TE}n}\right|^2 = \frac{2\pi\hbar c}{\Lambda}\frac{k_0^3}{n(n+1)}. \tag{3.5}$$

Here, $1-2q_n$ and $1-2p_n$ are the Mie reflection coefficients [89]; $z_1=\sqrt{\varepsilon}ka$; $z_2=ka$; $\varepsilon_1\equiv\varepsilon$ is the dielectric constant of the microsphere; and $\varepsilon_2=1$. Note that upon the normalisation of the wave functions the contribution from the region inside the dielectric microsphere is negligible compared to that from the region with $r\sim\Lambda$.

To study the interaction of the atomic oscillator with the continuum of the electromagnetic modes modified by the presence of the dielectric microsphere, one should also know the density of final states, i.e., the number of states of the electromagnetic field in the unit energy interval. The requirement for the disappearance of the tangential components of the electric field for the TM modes on the inner surface of the quantisation sphere leads to the transcendental equation

$$\frac{\mathrm{d}}{\mathrm{d}r}(rZ)\Big|_{r=\Lambda} = 0, \tag{3.6}$$

$$Z = \alpha^{(1)}_{\mathrm{TM}n}h^{(1)}_n\left(\frac{\omega_s}{c}r\right) + \alpha^{(2)}_{\mathrm{TM}n}h^{(2)}_n\left(\frac{\omega_s}{c}r\right),$$

which has asymptotic solutions

$$\omega_s = \left(\varkappa + \frac{n+1}{2}\right)\frac{\pi c}{\Lambda} + \ldots . \tag{3.7}$$

This means that the density of final states will be described by a simple expression

$$\rho_{\mathrm{TM}}(\omega) = \frac{\mathrm{d}\varkappa}{\mathrm{d}(\hbar\omega_s)} = \frac{\Lambda}{\pi\hbar c}, \tag{3.8}$$

which coincides with the density of final states in the absence of the microsphere. In the case of TE mode, the density of states is the same.

The independence of the density of final states in a large cavity (with radius $\Lambda \to \infty$) of the presence of the microsphere inside it is a corollary of the general theorem about the asymptotic distribution of eigenvalues [91], so that the change in the spectroscopic parameters of the atom located near meso- and nanostructures (of finite volume) is determined only by the properties of the transition matrix element and the wave functions of photons.

Having found the wave functions and densities of final states, we can immediately obtain the spontaneous decay rates from Eqn (2.15). By substituting Eqns (3.1), (3.2), and (3.8) into Eqn (2.15) and dividing the result by the spontaneous transition rate in a free space

$$\gamma_0 = \frac{4}{3}\frac{d^2k^3}{\hbar}, \tag{3.9}$$

we obtain the expressions for the rate of electric E_1 transitions with the radial orientation of the electric dipole moment ($r > a$) [73, 81]:

$$\left(\frac{\gamma}{\gamma_0}\right)_{\mathrm{rad}} = \frac{3}{2}\sum_{n=1}^{\infty} n(n+1)(2n+1) \times \left(\frac{|j_n(k_2 r) - q_n h_n^{(1)}(k_2 r)|}{k_2 r}\right)^2. \tag{3.10}$$

For the tangential orientation, we have

$$\left(\frac{\gamma}{\gamma_0}\right)_{\mathrm{tan}} = \frac{3}{2}\left[\sum_{n=1}^{\infty}\left(n+\frac{1}{2}\right)\left[\left|j_n(z') - p_n h_n^{(1)}(z')\right|^2\right] + \sum_{n=1}^{\infty}\left(n+\frac{1}{2}\right)\left|\frac{1}{z'}\frac{\mathrm{d}\left[z'\left(j_n(z') - q_n h_n^{(1)}(z')\right)\right]}{\mathrm{d}z'}\right|^2\right]_{z'=k_2 r}. \tag{3.11}$$

In the case of a sphere with the radius small compared to the emission wavelength, $ka \to 0$ (nanosphere), only the first term is substantial in Eqns (3.10) and (3.11), and we have

$$\left(\frac{\gamma}{\gamma_0}\right)_{\mathrm{rad}} \overset{ka\to 0}{\longrightarrow} \left|\frac{3\varepsilon}{\varepsilon+2}\right|^2, \tag{3.12}$$

$$\left(\frac{\gamma}{\gamma_0}\right)_{\mathrm{tan}} \overset{ka\to 0}{\longrightarrow} \left|\frac{3}{\varepsilon+2}\right|^2. \tag{3.13}$$

Fig. 5 shows the dependences of the decay rates on the sphere radius. In the region of small radii, the behaviour of the curves is determined by asymptotics (3.12) and (3.13). As the sphere radius increases, the resonance modes can be excited in the sphere (whispering gallery modes [18–20]). These modes are quite interesting, but their analysis is beyond the scope of our review devoted to nanoobjects, where such resonances are absent.

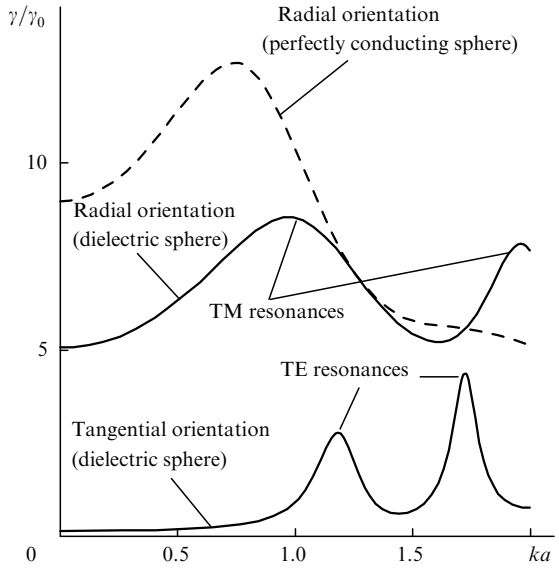

Figure 5. Dependences of the rate of dipole E_1 transitions of different orientations on ka for an atom located near a dielectric sphere ($\varepsilon = 6$) and a perfectly conducting sphere.

The case of a perfectly conducting (metal) surface is obtained if the dielectric constant ε in Eqns (3.10) and (3.11) tends to infinity. As a result, the expressions for the Mie coefficients are simplified:

$$q_{n\,\mathrm{met}} = \frac{\mathrm{d}}{\mathrm{d}z_2}[z_2 j_n(z_2)] \Big/ \frac{\mathrm{d}}{\mathrm{d}z_2}\left[z_2 h_n^{(1)}(z_2)\right]\Big|_{z_2=ka}, \tag{3.14}$$

$$p_{n\,\mathrm{met}} = \frac{j_n(ka)}{h_n^{(1)}(ka)}, \tag{3.15}$$

and the rates are described by expressions (3.10) and (3.11) in which the replacements $q_n \to q_{n\,\mathrm{met}}$ and $p_n \to p_{n\,\mathrm{met}}$ are made. On the surface of the metal sphere, the expressions for the rates are substantially simplified [90]:

$$\left(\frac{\gamma}{\gamma_0}\right)_{\mathrm{rad}} = \frac{3}{2(ka)^4}\sum_{n=1}^{\infty}\frac{n(n+1)(2n+1)}{\left|h_n^{(1)}(ka)\right|^2}, \tag{3.16}$$

$$\left(\frac{\gamma}{\gamma_0}\right)_{\mathrm{tan}} = 0. \tag{3.17}$$

In the case of an infinitely small conducting sphere, we have instead of Eqns (3.16) and (3.17)

$$\left(\frac{\gamma}{\gamma_0}\right)_{\mathrm{rad}} = 9, \tag{3.18}$$

$$\left(\frac{\gamma}{\gamma_0}\right)_{\mathrm{tan}} = 0. \tag{3.19}$$

respectively. These expressions are, of course, consistent with expressions (3.12) and (3.13).

So far, we considered a dielectric sphere without losses. However, a complete electrodynamic problem for this

sphere has an analytic solution and, therefore, we can consider the sphere with losses. In this case, the classical approach [expression (2.8)] is the most convenient. Then, the spontaneous decay rate for the transition with the radial orientation will have the form [73, 81]

$$\left(\frac{\gamma}{\gamma_0}\right)_{\text{rad}} = 1 - \frac{3}{2}\,\text{Re}\left[\sum_{n=1}^{\infty} n(n+1)(2n+1)q_n\left(\frac{h_n^{(1)}(kr)}{kr}\right)^2\right]. \qquad (3.20)$$

When the dielectric constant ε is real, expression (3.20) coincides with Eqn (3.10), whereas this is not the case for a sphere with inner losses. Expression (3.10) describes only radiative losses, whereas expression (3.20) takes into account Joule losses inside the sphere as well. For small spheres ($ka \to 0$), i.e., nanospheres, this difference becomes significant. Indeed, in this case the relative rate of radiative losses obtained from Eqn (3.10) is

$$\left(\frac{\gamma}{\gamma_0}\right)_{\text{rad}}^{\text{radiative}} \xrightarrow{ka\to 0} \left|1 + \frac{2(\varepsilon-1)}{\varepsilon+2}\left(\frac{a}{r}\right)^3\right|^2, \qquad (3.21)$$

whereas for the total rate we obtain from (3.20) the expression

$$\left(\frac{\gamma}{\gamma_0}\right)_{\text{rad}}^{\text{total}} \xrightarrow{ka\to 0} \text{Re}\left\{\left[1 + \frac{2(\varepsilon-1)}{\varepsilon+2}\left(\frac{a}{r}\right)^3\right]\right\} + \frac{3}{2(ka)^3}\left(\frac{a}{r}\right)^4 \text{Im}\sum_{n=1}^{\infty} n(n+1)\left(\frac{a}{r}\right)^{2n} \times\left[\frac{(\varepsilon-1)(n+1)}{\varepsilon n + n + 1} + \text{O}(ka^2)\right]. \qquad (3.22)$$

Comparison of expressions (3.21) and (3.22) shows that the total rate of losses contains the term, which infinitely (as $1/(ka)^3$) increases with decreasing the sphere radius. Moreover, one can see from Eqns (3.20) and (3.22) that the rate of nonradiative processes in the atom located near the surface ($r \to a$) of a sphere with losses tends to infinity. Fig. 6 shows the dependences of the rates of radiative and total losses for gold, silver, and diamond nanospheres with $ka = 0.2$. One can see that the loss rate increases when the atom approaches the nanosphere surface and that the radia-tive loss rate near the conducting nanosphere increases negligibly compared to the nonradiative (Joule) loss rate. Expressions (3.21) and (3.22) are valid in most practically important cases. However, there exists a region of parameters where these expressions cannot be applied. The case in point is the electromagnetic trap (plasmon resonance), when the condition $|\varepsilon + 2| \ll (ka)^2 \ll 1$ is fulfilled [94]. In particular, for a potassium sphere at the wavelength 578 nm and $\varepsilon = -2.46 + \text{i}0.295$, we have $|\varepsilon + 2| \approx 0.5$, and for $ka = 0.8$ the above condition is approximately fulfilled. It seems that in some situations this condition is even better fulfilled and $|\varepsilon + 2| \approx 0$. In this case, the Joule losses will be small, whereas the radiative losses and the decay rate will become very large (the upper curve in Fig. 6). For $\varepsilon \approx -2$, we have for nanospheres instead of expressions (3.21) and (3.22)

$$\left(\frac{\gamma}{\gamma_0}\right)_{\text{rad}}^{\text{radiative}} \xrightarrow{\varepsilon=-2,\, ka\to 0} \frac{25}{4(ka)^4}\left(\frac{a}{r}\right)^6 + \ldots. \qquad (3.23)$$

Note that these relations are only valid under conditions of the plasmon resonance and we are not aware of materials that would provide the conditions for the existence of this resonance in spheres. The case of spheroidal particles is more favourable for the resonance existence (see section 5 below).

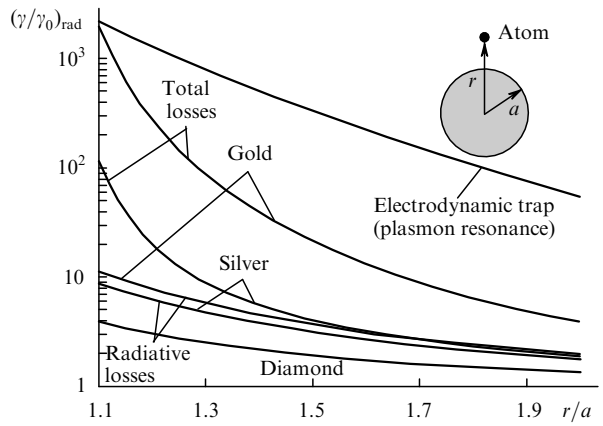

Figure 6. Dependences of the rates of dipole E_1 transitions on the distance of an atom from the surface of diamond ($\varepsilon = 6$), gold ($\varepsilon = -8.37 + \text{i}1.16$, $\lambda = 600$ nm [92]), and silver ($\varepsilon = -15.37 + \text{i}0.231$, $\lambda = 632.8$ nm [93]) nanospheres.

As a whole, a sphere of size that is small compared to the emission wavelength (nanosphere) substantially affects the decay of the excited state of an atom. In the case of a dielectric nanosphere (small inner losses, $\varepsilon'' \ll \varepsilon'$), the excitation energy is emitted as photons, the radiative decay rate being several times increased or decreased depending on the orientation of the transition dipole moment. In the case of a metal nanosphere (large inner losses), the energy of the excited atom is mainly dissipated inside the nanosphere; the rate of this nonradiative process substantially increases both with decreasing sphere radius and when the atom is approaching the sphere surface. In a special case (plasmon resonance, $\varepsilon \approx -2$), the decay is still radiative (the energy escapes to infinity as photons), but its rate is inversely proportional to the fourth degree of the sphere radius.

4. Spontaneous emission of an atom located near an infinite circular cylinder

The case of a cylinder is more complicated and the number of papers devoted to its study is much smaller. A classical problem on emission of currents arbitrarily distributed near a conducting cylinder was considered in paper [95]. The method for solving a classical problem on a dipole located on the dielectric cylinder axis was proposed in paper [96]. More detailed studies were performed in papers [97–99] where the main attention was paid to numerical calculations. The case of dipole and quadrupole transitions in an atom located near a perfectly conducting cylinder was studied in detail, both analytically and numerically in paper [57].

In the cylindrical case, it is also convenient to use the quantum-mechanical approach to the problem in which a cylinder and an atom are surrounded by a coaxial perfectly

conducting surface of radius Λ and length L. In fact, the total system represents a coaxial resonator of limited length. The geometry of the problem is shown in Fig. 7. In this case, the expressions for the electric field strength $\boldsymbol{e}(\boldsymbol{s}, \boldsymbol{r})$ of the sth TM mode in terms of Bessel functions have the form [100]

$$e_z = C_{\mathrm{TM}} v^2 [J_m(v\rho) - Y_m(v\rho) q_{\mathrm{TM}}(m, v\Lambda)] \mathrm{e}^{\mathrm{i}m\varphi} \cos(hz),$$

$$e_\rho = -C_{\mathrm{TM}} vh [J'_m(v\rho) - Y'_m(v\rho) q_{\mathrm{TM}}(m, v\Lambda)] \mathrm{e}^{\mathrm{i}m\varphi} \sin(hz), \quad (4.1)$$

$$e_\varphi = \frac{-\mathrm{i} C_{\mathrm{TM}} hm}{\rho} [J_m(v\rho) - Y_m(v\rho) q_{\mathrm{TM}}(m, v\Lambda)] \mathrm{e}^{\mathrm{i}m\varphi} \sin(hz),$$

where the prime denotes a derivative with respect to the argument; h is the longitudinal wave number; v is the radial wave number;

$$q_{\mathrm{TM}}(m, v\Lambda) = \frac{J_m(v\Lambda)}{Y_m(v\Lambda)}; \qquad C_{\mathrm{TM}} = \left\{ \frac{4\pi\hbar\omega_{\boldsymbol{s}}}{L\Lambda v [1 + q^2_{\mathrm{TM}}(m, v\Lambda)] k^2} \right\}^{1/2}. \quad (4.2)$$

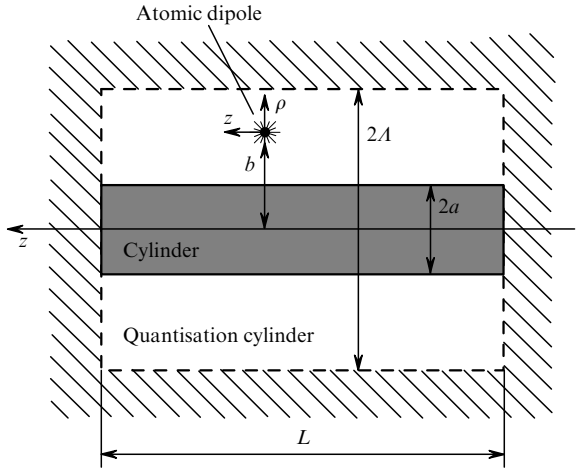

Figure 7. Geometry of a cylindrical case.

Expression (4.1) provides the fulfilment of the boundary conditions for TM modes on the cylinder surface ($r = a$) for any h and v. To provide the fulfilment of the boundary conditions on the quantisation cylinder surface ($z = 0, L$; $r = \Lambda$), the quantities h and v should satisfy the following conditions

$$h = \frac{\pi n_z}{L}, \quad n_z = 0, 1, 2, \ldots, \qquad J_m(v\Lambda) - Y_m(v\Lambda) q_{\mathrm{TM}}(m, v\Lambda) = 0. \quad (4.3)$$

In the limit $\Lambda \to \infty$, the second equation in (4.3) has the asymptotic solution

$$v = \frac{\pi}{\Lambda} \left(n_\rho + \frac{m}{2} + \frac{1}{4} \right) + \ldots, \quad n_\rho = 0, 1, 2, \ldots. \quad (4.4)$$

A set of quantum numbers m, n_z, n_ρ forms the vector index $\boldsymbol{s} = \{m, n_z, n_\rho\}$ for the TM modes, which was used above.

The transverse electric modes are quantised similarly to the TM modes.

The limited coaxial resonator under study, which is formed by the cylinder and the quantisation volume, has the so-called fundamental modes along with the modes considered above [100]. In our case, however, the fundamental modes do not contribute to the spontaneous decay rate in the limit $\Lambda \to \infty$.

In the case of a cylindrical geometry, the fundamental mode frequencies are determined by the well-known expression

$$\omega_{\boldsymbol{s}} = c\left(v^2 + h^2\right)^{1/2}, \quad (4.5)$$

where h and v are determined by quantisation conditions (4.3) and (4.4).

To find the spontaneous decay rates in accordance with the Fermi golden rule, the density of final states should be also known. It follows from Eqn (4.5) that the density of final states is determined by the following simple expression:

$$\rho_{\mathrm{TM}}(\omega) = \delta[\omega - \omega_{\boldsymbol{s}}(n_z, n_\rho)] \frac{\mathrm{d}n_z \mathrm{d}n_\rho}{\hbar}$$

$$= \delta\left[\omega - c\left(h^2 + v^2\right)^{1/2}\right] \frac{L\Lambda \mathrm{d}h \mathrm{d}v}{\pi^2\hbar} = \frac{L\Lambda}{\pi^2\hbar c} \frac{k}{v} \mathrm{d}h. \quad (4.6)$$

In deriving expression (4.6), we have passed in a usual way from discrete variables n_z, n_ρ to continuous wave numbers h and v. As a result, only the longitudinal wave number is an independent variable, which characterises the final state, and we should perform integration with respect to this number. The radial wave number is determined by the relation $v = (k^2 - h^2)^{1/2}$. In the case of the TE modes, the density of states is the same.

By substituting the found density of final states into Eqn (2.15), we obtain the expression for the spontaneous transition rate for the atom located at the point $\boldsymbol{r}_0 = (b, 0, 0)$:

$$\gamma_{\mathrm{dip}} = \frac{L\Lambda}{\pi\hbar^2 c} \left[\sum_{m=-\infty}^{m=\infty} \int_0^k |\boldsymbol{e}_{\mathrm{TM}}(m, \boldsymbol{r}_0)\boldsymbol{d}|^2 \frac{k}{v} \mathrm{d}h + \sum_{m=-\infty}^{m=\infty} \int_0^k |\boldsymbol{e}_{\mathrm{TE}}(m, \boldsymbol{r}_0)\boldsymbol{d}|^2 \frac{k}{v} \mathrm{d}h \right]. \quad (4.7)$$

By substituting into Eqn (4.7) expressions (4.1) for particular photon wave functions and their analogues for TE modes, we obtain the expressions for spontaneous decay rates for arbitrary orientations of the dipole moment [57]:

$$\frac{\gamma_\rho}{\gamma_0} = \frac{3}{2} \sum_{n=-\infty}^{\infty} \int_0^k \mathrm{d}h \frac{h^2}{k^3} \left| \frac{\mathrm{d}}{\mathrm{d}z} J_n(z) \Big|_{z=vb} - \frac{J_n(v\Lambda)}{H_n^{(1)}(v\Lambda)} \frac{\mathrm{d}}{\mathrm{d}z} H_n^{(1)}(z) \Big|_{z=vb} \right|^2 + \frac{3}{2} \sum_{n=-\infty}^{\infty} \int_0^k \mathrm{d}h \frac{n^2}{k(vb)^2} \quad (4.8)$$

$$\times \left| J_n(vb) - \left[\frac{\mathrm{d}}{\mathrm{d}z} J_n(z) \Big|_{z=v\Lambda} \Big/ \frac{\mathrm{d}}{\mathrm{d}z} H_n^{(1)}(z) \Big|_{z=v\Lambda} \right] H_n^{(1)}(vb) \right|^2,$$

$$\frac{\gamma_\varphi}{\gamma_0}=\frac{3}{2}\sum_{n=-\infty}^{\infty}\int_0^k \mathrm{d}h\,\frac{h^2n^2}{k(kb)^2v^2}\left|J_n(vb)\right.$$

$$\left.-\frac{J_n(va)}{H_n^{(1)}(va)}H_n^{(1)}(vb)\right|^2+\frac{3}{2}\sum_{n=-\infty}^{\infty}\int_0^k\frac{\mathrm{d}h}{k}\left|\frac{\mathrm{d}}{\mathrm{d}z}J_n(z)\right|_{z=vb} \quad (4.9)$$

$$-\left[\frac{\mathrm{d}}{\mathrm{d}z}J_n(z)\right|_{z=va}\Big/\frac{\mathrm{d}}{\mathrm{d}z}H_n^{(1)}(z)\Big|_{z=va}\Big]\frac{\mathrm{d}}{\mathrm{d}z}H_n^{(1)}(z)\Big|_{z=vb}\Big|^2,$$

$$\frac{\gamma_z}{\gamma_0}=\frac{3}{2}\sum_{n=-\infty}^{\infty}\int_0^k \mathrm{d}h\,\frac{v^2}{k^3}\left|J_n(vb)-\frac{J_n(va)}{H_n^{(1)}(va)}H_n^{(1)}(vb)\right|^2. \quad (4.10)$$

Fig. 8 shows spontaneous decay rates as functions of the distance between the atom and the cylinder for different orientations of the atomic dipole moment. One can see that the most strong changes occur when the atom is located very close to the cylinder surface ($b\to a$). In this case, it follows from (4.9) and (4.10) that the spontaneous decay rates for tangential orientations of the dipole are zero for any radius of the cylinder (one can also see this in Fig. 8).

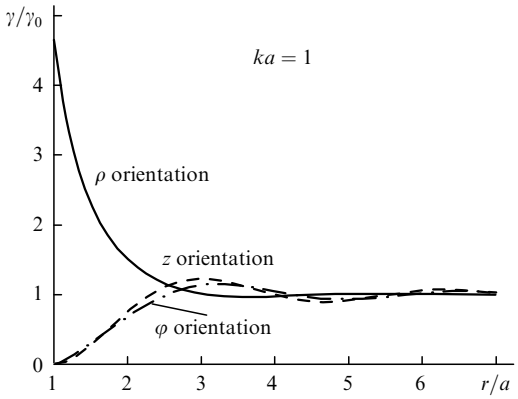

Figure 8. Rates of the dipole E_1 transitions in an atom located near the surface of a perfectly conducting cylinder as functions of the atom position for different orientations of the dipole moment.

On the other hand, the spontaneous transition rate in the atom on the cylinder surface ($a=b$) with the radial orientation of the dipole moment substantially increases compared to the case of a free space and can be written in the form [57]

$$\frac{\gamma_\rho}{\gamma_0}=\frac{6}{\pi^2}\sum_{n=-\infty}^{\infty}\int_0^k \mathrm{d}h\,\frac{h^2}{k^3(va)^2}\,\frac{1}{\left|H_n^{(1)}(va)\right|^2}$$

$$+\frac{6}{\pi^2}\sum_{n=-\infty}^{\infty}\int_0^k \mathrm{d}h\,\frac{n^2}{k(va)^4}\left|\frac{\mathrm{d}}{\mathrm{d}z}H_n^{(1)}(z)\Big|_{z=va}\right|^{-2}. \quad (4.11)$$

Moreover, when the cylinder radius tends to zero, the spontaneous decay rate of the atom with the radial orientation of the dipole moment tends to infinity. In the limit $ka=kb\to 0$, the TM mode with $n=0$ makes the main contribution into Eqn (4.11) [57]:

$$\frac{\gamma_\rho}{\gamma_0}\overset{kb=ka\to 0}{\longrightarrow}\frac{3}{2(ka)^2}\left[1+\frac{2}{\pi}\arctan L^*\right.$$

$$\left.+\frac{4(\ln 2-1)}{\pi^2(1+L^{*2})}+\ldots\right]+4+\ldots,$$

$$L^*=\frac{2}{\pi}\left(\ln\frac{ka}{2}+\gamma\right),\quad \gamma=0.5772\,. \quad (4.12)$$

Such behaviour has no analogue in the case of a perfectly conducting sphere of small radius, when the decay rate remains finite. Physically, this effect is explained by the fact that the radial dipole excites in the cylinder a current wave which weakly decays with distance and is a source of a high-power radiation. Fig. 9 shows the dependences of the spontaneous decay rates of the atom on its distance to the cylinder, sphere, and plane surfaces. One can see that the decay rate most strongly increases near the cylinder surface, while near the perfectly conducting plane the increase in the decay rate is minimal.

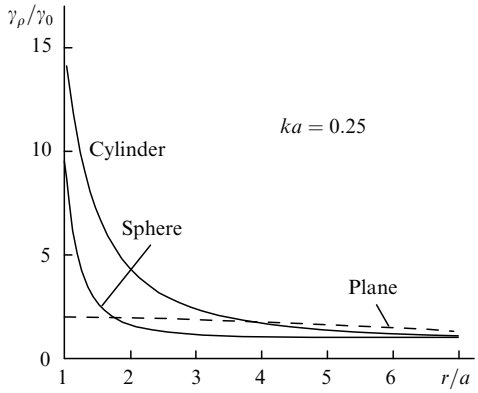

Figure 9. Rates of the dipole E_1 transitions in an atom located near different surfaces as functions of the atom position for the radial orientation of the dipole moment.

The problem on a dielectric cylinder can be solved similarly to the case of a perfectly conducting cylinder, which was considered above. A complete solution is rather cumbersome, however, when the cylinder radius is small compared to the emission wavelength (nanocylinder), simple asymptotics can be obtained (an atom located on the surface, radial orientation) [101]:

$$\frac{\gamma_\rho}{\gamma_0}=\left(\frac{2\varepsilon}{\varepsilon+1}\right)^2$$

$$+\frac{\varepsilon^2(\varepsilon-1)\{15\varepsilon^2+60\varepsilon+2201-1680[\gamma+\ln(ka)]\}(ka)^2}{300(\varepsilon+1)^3}$$

$$+\frac{12}{(ka)^4}\,\frac{\varepsilon-1}{\varepsilon+1}\exp\left[-\frac{2}{(ka)^2}\,\frac{\varepsilon+1}{\varepsilon-1}+\frac{\varepsilon+1}{4}-2\gamma\right]. \quad (4.13)$$

The exponentially small term in this expression is related to the fundamental mode existing in a dielectric cylinder of an arbitrarily small thickness [102]. Fig. 10 shows the dependences of the decay rates on the distance from the atom to the cylinder surface for different dielectric constants.

As a whole, a nanocylinder strongly affects the excited-state decay in the atom. In the case of a perfectly conducting cylinder, the decay is purely radiative and its rate can in-

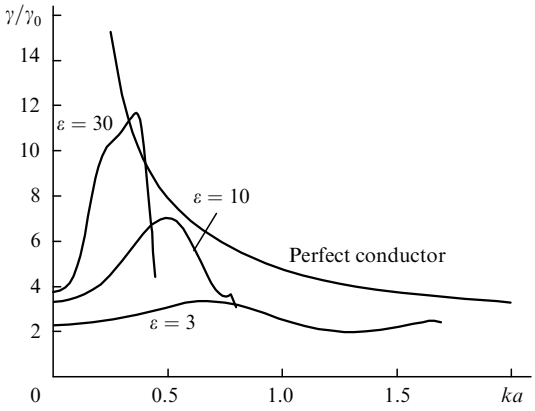

Figure 10. Rates of the dipole E_1 transitions in an atom located near the surface of a dielectric cylinder as functions of the atom position for different dielectric constants and the radial orientation of the dipole moment.

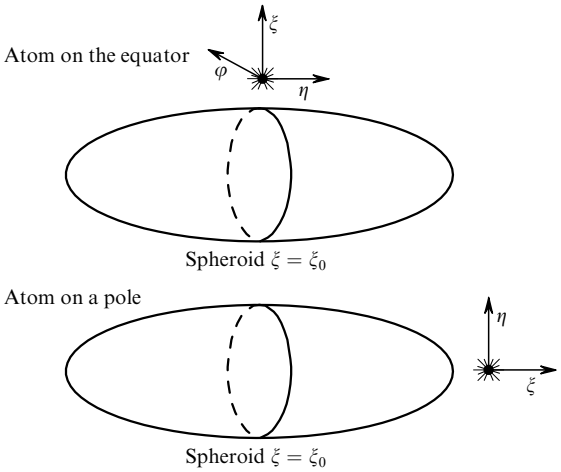

Figure 11. Geometry of the problem on spontaneous emission of an atom located near a prolate spheroid.

crease infinitely with decreasing cylinder radius (radial orientation of the transition dipole moment). In the case of a dielectric cylinder, the decay is more complicated: a fraction of the energy is emitted to infinity as photons, while the remaining fraction is transformed to the energy of undamped waveguide modes of the cylinder and, hence, is not emitted. In the case of a dielectric cylinder of small radius, the intensities of nonradiative processes are exponentially small.

The general case of a cylinder with losses has not been studied in detail. However, in this case, as for a sphere, the imaginary part of the dielectric constant also causes a substantial increase in the nonradiative decay rate and in the total decay rate. Spontaneous emission of an atom in the case of a plasmon resonance in the cylinder (the dielectric constant $\varepsilon \approx -1$) also has not been studied; however, it is clear that in this case the radiative decay rates also will be substantially greater.

5. Spontaneous emission of an atom located near a dielectric prolate spheroid

The case of a dielectric spheroid attracts a special attention because a dielectric microsphere and a cylinder considered above are particular cases of a prolate spheroid. A classical problem of scattering of plane waves by dielectric spheroids has been studied in Refs [103, 104]. A particular problem on the axially symmetric emission near a perfectly conducting spheroid has been considered in Ref. [105]. However, as far as we know, the problem on spontaneous emission of an atom located near a dielectric nanospheroids has not been solved.

In this connection we consider the case of a small (compared to the wavelength) prolate spheroid assuming that an atom is located near the spheroid. The geometry of the problem is shown in Fig. 11. In this case, according to expression (2.9), the spontaneous decay rate is determined by the total dipole moment of the system. The total dipole moment can be found by solving the quasi-static problem

$$\mathrm{rot}\boldsymbol{E} = 0, \ \mathrm{div}\boldsymbol{D} = 4\pi\rho, \tag{5.1}$$

where the density of the dipole charge is determined by the usual expression

$$\rho = -(\boldsymbol{d}_0)\delta(\boldsymbol{r} - \boldsymbol{r}')\mathrm{e}^{-\mathrm{i}\omega t}. \tag{5.2}$$

Hereafter, we will not specify the time dependence of the fields.

By introducing the potential $\tilde{\varphi}$ with the help of the expression

$$\boldsymbol{E} = -\nabla(\boldsymbol{d}_0\nabla')\tilde{\varphi}(\boldsymbol{r}, \boldsymbol{r}') \tag{5.3}$$

we obtain instead of (5.1)

$$-\nabla^2\tilde{\varphi} = 4\pi\delta(\boldsymbol{r} - \boldsymbol{r}') \text{ outside the spheroid;}$$
$$-\nabla^2\tilde{\varphi} = 0 \qquad \text{inside the spheroid.} \tag{5.4}$$

At the interface, the continuity conditions should be satisfied for normal components $\boldsymbol{D}$ and tangential components $\boldsymbol{E}$.

The solution of the problem (5.4) can be conveniently represented in the form

$$\tilde{\varphi} = \varphi_0 + \varphi_2 \text{ outside the spheroid;}$$
$$\tilde{\varphi} = \varphi_1 \qquad \text{inside the spheroid,} \tag{5.5}$$

where

$$\varphi_0 = \frac{1}{|\boldsymbol{r} - \boldsymbol{r}'|} \tag{5.6}$$

is the potential in a free space.

It is reasonable to solve the electrostatic problem (5.4)–(5.6) for a prolate spheroid in prolate spheroidal coordinates, in which the z axis coincides with the axis of the system. The relation between spheroidal and Cartesian coordinates has the form [106]

$$x = f[(1 - \eta^2)(\xi^2 - 1)]^{1/2}\cos\varphi,$$
$$y = f[(1 - \eta^2)(\xi^2 - 1)]^{1/2}\sin\varphi, \tag{5.7}$$
$$z = f\xi\eta.$$

The parameter ξ is an analogue of the radius in a spherical coordinate system and determines the ratio of the minor axis a of a spheroid to its major axis b:

$$\frac{b}{a}=\frac{(\xi^2-1)^{1/2}}{\xi}. \tag{5.8}$$

The Lamé parameters in this coordinate system have the form

$$g_\xi = f\left(\frac{\xi^2-\eta^2}{\xi^2-1}\right)^{1/2},\quad g_\eta = f\left(\frac{\xi^2-\eta^2}{1-\eta^2}\right)^{1/2},$$
$$g_\varphi = f[(1-\eta^2)(\xi^2-1)]^{1/2}. \tag{5.9}$$

The Green function (5.6) in a free space can be represented in the form [106]

$$\varphi_0=\frac{1}{|\boldsymbol{r}-\boldsymbol{r}'|}=\frac{1}{f}\sum_{n=0}^{\infty}\sum_{m=0}^{n}(2-\delta_{m0})(-1)^m(2n+1)\left[\frac{(n-m)!}{(n+m)!}\right]^2 \tag{5.10}$$
$$\times P_n^m(\eta)P_n^m(\eta')\cos m(\varphi-\varphi')\begin{cases} P_n^m(\xi)Q_n^m(\xi'), & \xi<\xi',\\ P_n^m(\xi')Q_n^m(\xi), & \xi>\xi'\end{cases}$$

In Eqn (5.10) and below, P and Q are the associated Legendre polynomials of the first and second kind, respectively [107]. The associated polynomials with the argument η are defined on the cut $-1<\eta<1$, while the associated polynomials with the argument $\xi>1$ have the cut from $-\infty$ to 1.

Expansion Eqn (5.10) can be conveniently represented in the form

$$\varphi_0^{<}=\sum_{n=0}^{\infty}\sum_{m=0}^{n}P_n^m(\eta)P_n^m(\xi)$$
$$\times(\alpha_{nm}^{0<}\cos m\varphi+\beta_{nm}^{0<}\sin m\varphi),\quad \xi<\xi', \tag{5.11}$$
$$\varphi_0^{>}=\sum_{n=0}^{\infty}\sum_{m=0}^{n}P_n^m(\eta)Q_n^m(\xi)$$
$$\times(\alpha_{nm}^{0>}\cos m\varphi+\beta_{nm}^{0>}\sin m\varphi),\quad \xi>\xi',$$

where the coefficients $\alpha_{nm}^{0\lessgtr}$, $\beta_{nm}^{0\lessgtr}$ have the form

$$\begin{Bmatrix}\alpha_{nm}^{0<}\\ \beta_{nm}^{0<}\end{Bmatrix}=(2-\delta_{m0})(-1)^m(2n+1)\left[\frac{(n-m)!}{(n+m)!}\right]^2$$
$$\times P_n^m(\eta')Q_n^m(\xi')\begin{Bmatrix}\cos m\varphi\\ \sin m\varphi\end{Bmatrix}, \tag{5.12}$$
$$\begin{Bmatrix}\alpha_{nm}^{0>}\\ \beta_{nm}^{0>}\end{Bmatrix}=(2-\delta_{m0})(-1)^m(2n+1)\left[\frac{(n-m)!}{(n+m)!}\right]^2$$
$$\times P_n^m(\eta)P_n^m(\xi')\begin{Bmatrix}\cos m\varphi\\ \sin m\varphi\end{Bmatrix}. \tag{5.13}$$

We will seek the solution of the problem (5.4)–(5.6) in the region $\xi_0<\xi<\xi'$ (between the spheroid and dipole) in the form

$$\tilde\varphi=\sum_{n=0}^{\infty}\sum_{m=0}^{n}P_n^m(\eta)P_n^m(\xi)(\alpha_{nm}^{0<}\cos m\varphi+\beta_{nm}^{0<}\sin m\varphi)$$
$$+\sum_{n=0}^{\infty}\sum_{m=0}^{n}P_n^m(\eta)Q_n^m(\xi)(\alpha_{nm}^{(2)}\cos m\varphi+\beta_{nm}^{(2)}\sin m\varphi), \tag{5.14}$$

and in the region $1<\xi<\xi_0$ (inside the spheroid) in the form

$$\tilde\varphi=\sum_{n=0}^{\infty}\sum_{m=0}^{n}P_n^m(\eta)P_n^m(\xi)\left(\alpha_{nm}^{(1)}\cos m\varphi+\beta_{nm}^{(1)}\sin m\varphi\right). \tag{5.15}$$

The continuity condition for the tangential components of the field and the normal components of the induction allow us to find the coefficients determining the fields outside the spheroid:

$$\alpha_{nm}^{(2)}=(\varepsilon-1)P_n^m(\xi_0)P_n^{m'}(\xi_0)\left[Q_n^{m'}(\xi_0)P_n^m(\xi_0)\right.$$
$$\left.-\varepsilon P_n^{m'}(\xi_0)Q_n^m(\xi_0)\right]^{-1}\alpha_{nm}^{0<}=G_{nm}\alpha_{nm}^{0<}, \tag{5.16}$$
$$\beta_{nm}^{(2)}=G_{nm}\beta_{nm}^{0<}.$$

Note that expressions (5.16) become infinite for some real values of the dielectric constant, so that our quasi-static problem has no solution. In this case, as in the case of a dielectric sphere, an electrodynamic trap appears (plasmon resonance), which can be described only within the framework of the complete electrodynamic theory. It is obvious that the decay rate substantially increases in this case. We will analyse this case below.

Taking Eqns (5.11) and (5.14) into account, the total potential at large distances from the dipole takes the form

$$\tilde\varphi^{>}=\sum_{n=0}^{\infty}\sum_{m=0}^{n}P_n^m(\eta)Q_n^m(\xi)\left[\left(\alpha_{nm}^{0>}+G_{nm}\alpha_{nm}^{0<}\right)\cos m\varphi\right.$$
$$\left.+\left(\beta_{nm}^{0>}+G_{nm}\beta_{nm}^{0<}\right)\sin m\varphi\right],\ \xi>\xi'. \tag{5.17}$$

To find the spontaneous decay rate according to (2.9), we should find the total dipole moment of the system. For this purpose, we find the asymptotics of Eqn (5.17) at large distances from the spheroid and the dipole, i.e., for $\xi\to\infty$. One can easily see that the terms with $n=1$ (dipole radiation) make the dominant contribution in this region:

$$\tilde\varphi^{>}\approx\frac{1}{\xi f}+\frac{1}{\xi^2 f}\left[P_1(\eta')P_1(\xi')\left(1+G_{10}\frac{Q_1(\xi')}{P_1(\xi')}\right)\cos\theta\right.$$
$$\left.+P_1^1(\eta')P_1^1(\xi')\left(1+G_{11}\frac{Q_1^1(\xi')}{P_1^1(\xi')}\right)\sin\theta\cos(\varphi-\varphi')\right]. \tag{5.18}$$

The dipole potential has the form

$$\varphi^{>}=(\boldsymbol{d}_0\nabla')\tilde\varphi^{>}. \tag{5.19}$$

By differentiating this expression and comparing the result with the expression for the dipole potential

$$\varphi_{\rm dip}=\frac{\boldsymbol{d}_{\rm tot}\boldsymbol{R}}{R^3}, \tag{5.20}$$

we can find the total dipole moment of the system and,

taking Eqn (2.9) into account, the change in the spontaneous decay rate. For the orientation of the dipole moment along axes ξ, η, and φ, we have [108]

$$\frac{\gamma_\xi}{\gamma_0} = \frac{\xi^2-1}{\xi^2-\eta^2}\left\{\eta^2[1+G_{10}Q_1'(\xi)]^2 + (1-\eta^2)\left[\frac{\xi}{(\xi^2-1)^{1/2}} + G_{11}Q_1^{1\prime}(\xi)\right]^2\right\}, \tag{5.21}$$

$$\frac{\gamma_\eta}{\gamma_0} = \left[\eta^2(\xi^2-1)\left(1+G_{11}\frac{Q_1^1(\xi)}{(\xi^2-1)^{1/2}}\right)^2 + (1-\eta^2)\xi^2\left(1+G_{10}\frac{Q_1(\xi)}{\xi}\right)^2\right](\xi^2-\eta^2)^{-1}, \tag{5.22}$$

$$\frac{\gamma_\varphi}{\gamma_0} = \left(1+G_{11}\frac{Q_1^1(\xi)}{(\xi^2-1)^{1/2}}\right)^2. \tag{5.23}$$

In expressions (5.21)–(5.23) and below, we omit the prime at the variables describing the atom position.

The coefficients G_{10} and G_{11} are determined by expression (5.16) and have the form

$$G_{10} = \frac{(\varepsilon-1)\xi_0}{Q_1'(\xi_0)\xi_0 - \varepsilon Q_1(\xi_0)}, \qquad G_{11} = \frac{(\varepsilon-1)\xi_0}{Q_1^{1\prime}(\xi_0)(\xi_0^2-1)^{1/2} - \varepsilon\xi_0 Q_1'(\xi_0)}. \tag{5.24}$$

From the physical point of view, the following particular cases are of interest: an atom located on the spheroid pole ($\eta = 1$), an atom located on the spheroid equator ($\eta = 0$), the limiting case of a sphere ($\xi_0 = \infty$), the limiting case of a tip ($\xi_0 = 0$) and, finally, the limiting case of a perfectly conducting plane.

When an atom is located on the pole ($\eta = 1$), expressions (5.21)–(5.23) are simplified:

$$\frac{\gamma_{\xi,\eta=1}}{\gamma_0} = \left[1+G_{10}\frac{\mathrm{d}}{\mathrm{d}\xi}Q_1(\xi)\right]^2, \tag{5.25}$$

$$\frac{\gamma_{\eta,\eta=1}}{\gamma_0} = \frac{\gamma_{\varphi,\eta=1}}{\gamma_0} = \left[1+G_{11}\frac{\mathrm{d}}{\mathrm{d}\xi}Q_1(\xi)\right]^2. \tag{5.26}$$

When an atom is located on the equator ($\eta = 0$), we have

$$\frac{\gamma_{\xi,\eta=0}}{\gamma_0} = \left[1+G_{11}\frac{\mathrm{d}}{\mathrm{d}\xi}Q_1^1(\xi)\frac{(\xi^2-1)^{1/2}}{\xi}\right]^2 \tag{5.27}$$

$$\frac{\gamma_{\eta,\eta=0}}{\gamma_0} = \left[1+G_{10}\frac{Q_1(\xi)}{\xi}\right]^2, \tag{5.28}$$

$$\frac{\gamma_{\varphi,\eta=0}}{\gamma_0} = \left[1+G_{11}\frac{\mathrm{d}}{\mathrm{d}\xi}Q_1(\xi)\right]^2. \tag{5.29}$$

The most interesting feature of the spontaneous decay rate for the dipole orientation along the φ axis is the independence of this rate of the coordinate η for any spheroid. By the way, this also follows from general expression (5.23). Dependences (5.25)–(5.29) for nanospheroid with $\xi_0 = 1.1$ are shown in Fig. 12. One can see that, as in the case of a sphere, the radial orientation of the dipole moment results in a stronger increase in the decay rate.

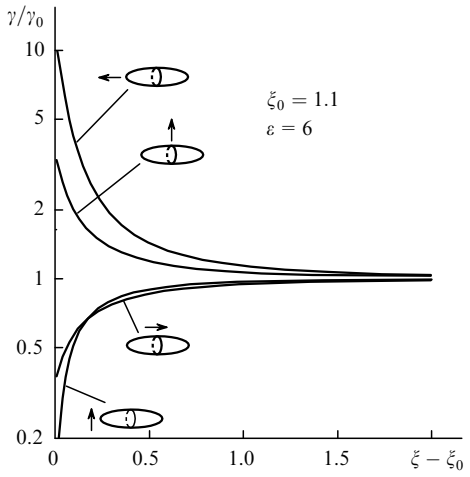

Figure 12. Rates of the dipole E_1 transitions in an atom located near the nanospheroid surface as functions of $\xi - \xi_0$ for different orientations of the dipole moment ($\xi_0 = 1.1$, $\varepsilon = 6$)

The results can be further simplified if we assume that the atom is located very close to the spheroid surface ($\xi \to \xi_0$). In this case, we obtain instead of Eqns (5.25)–(5.29) for the atom on the pole ($\eta = 1$)

$$\frac{\gamma_{\xi,\eta=1}}{\gamma_0} = \left\{2\varepsilon\left[\xi_0(\varepsilon-1)(\xi_0^2-1)\ln\frac{\xi_0+1}{\xi_0-1} + 2(\varepsilon+\xi_0^2-\xi_0^2\varepsilon)\right]^{-1}\right\}^2, \tag{5.30}$$

$$\frac{\gamma_{\eta,\eta=1}}{\gamma_0} = \frac{\gamma_{\varphi,\eta=1}}{\gamma_0} = \left\{4\left[\xi_0(\varepsilon-1)(\xi_0^2-1)\ln\frac{\xi_0+1}{\xi_0-1} + 2(\xi_0^2-\xi_0^2\varepsilon-2)\right]-1\right\}^2. \tag{5.31}$$

In the case of the atom located on the equator ($\eta = 0$), we have

$$\frac{\gamma_{\xi,\eta=0}}{\gamma_0} = \left\{4\varepsilon\left[\xi_0(\varepsilon-1)(\xi_0^2-1)\ln\frac{\xi_0+1}{\xi_0-1} + 2(\xi_0^2-\xi_0^2\varepsilon-2)\right]^{-1}\right\}^2, \tag{5.32}$$

$$\frac{\gamma_{\eta,\eta=0}}{\gamma_0} = \left\{2\left[\xi_0(\varepsilon-1)(\xi_0^2-1)\ln\frac{\xi_0+1}{\xi_0-1} + 2(\varepsilon+\xi_0^2-\xi_0^2\varepsilon)\right]^{-1}\right\}^2. \tag{5.33}$$

$$\frac{\gamma_{\varphi,\eta=0}}{\gamma_0} = \frac{\gamma_{\varphi,\eta=1}}{\gamma_0}. \tag{5.34}$$

These expressions demonstrate that decay rates (5.30) exceed decay rates (5.33) by a factor of ε^2 for spheroids of any shape. A similar relation takes place for Eqns (5.32) and (5.31), (5.34).

The expressions presented above are valid for spheroids of any shape. The decay rates for different positions and orientations of an atom can be easily obtained for a sphere

($\xi_0 \to \infty$) and a thin tip ($\xi_0 \to 1$) from expressions (5.30)–(5.34). For clarity, various results are summarised in Table 1, which demonstrates that the decay rates in the case of a spherical geometry completely coincide with the exact solution of the problem on the dipole emission in the presence of a dielectric sphere [81].

Table 1. Relative rates of radiative losses in an atomic oscillator located on the spheroid surface for different orientations, positions, materials, and shapes of the spheroid.

Geometry		Atom on a pole		Atom on the equator	
Dipole orientation	Shape	Dielectric	Metal ($\varepsilon \to \infty$)	Dielectric	Metal ($\varepsilon \to \infty$)
ξ	sphere	$\left\lvert\frac{3\varepsilon}{2+\varepsilon}\right\rvert^2$	9	$\left\lvert\frac{3\varepsilon}{2+\varepsilon}\right\rvert^2$	9
	needle	$\lvert\varepsilon\rvert^2$	$\left[\left(\ln\frac{2}{\xi_0-1}-2\right)(\xi_0-1)\right]^{-2}$	$\left\lvert\frac{2\varepsilon}{1+\varepsilon}\right\rvert^2$	4
η	sphere	$\left\lvert\frac{3}{2+\varepsilon}\right\rvert^2$	0	$\left\lvert\frac{3}{2+\varepsilon}\right\rvert^2$	0
	needle	$\left\lvert\frac{2}{1+\varepsilon}\right\rvert^2$	0	1	0
φ	sphere	$\left\lvert\frac{3}{2+\varepsilon}\right\rvert^2$	0	$\left\lvert\frac{3}{2+\varepsilon}\right\rvert^2$	0
	needle	$\left\lvert\frac{2}{1+\varepsilon}\right\rvert^2$	0	$\left\lvert\frac{2}{1+\varepsilon}\right\rvert^2$	0

A comparison with the results of the study of the dipole emission in the presence of an infinite circular cylinder [57, 101] is more interesting. In the case of a dielectric cylinder of small radius, the relative decay rates completely coincide with the rates near (on the equator) a strongly prolate spheroid (except the terms tending to zero with decreasing cylinder radius). This coincidence additionally confirms the correctness of our calculations.

As for a perfectly conducting cylinder, in the case of the radial orientation (ξ orientation), the results for a cylinder and a tip do not coincide. In the case of a perfectly conducting cylinder of infinitesimal radius, the decay rate infinitely increases, in accordance with (4.16), whereas for a perfectly conducting tip, we have

$$\frac{\gamma_\xi}{\gamma_0} \to 4. \tag{5.35}$$

This difference is explained by the fact that in the case of an infinite cylinder a current wave is excited in the region whose dimensions substantially exceed the emission wavelength [57], so that the quasi-static approximation cannot be used.

Of special interest is the study of a dipole oriented along the ξ axis and located on the spheroid pole (an atom located near the nanoscope tip). One can see from Table 1 that the relative decay rate increases quadratically with increasing dielectric constant. In the case of a perfect conduction, the decay rate increases infinitely as the spheroid is transformed to a infinitesimally thin needle. It is quite clear from the physical point of view because strong fields always appear on the spike.

In all other cases, a passage to a perfect conductivity is achieved by directing the dielectric constant to infinity. In this case, the decay rates for tangential orientations of the dipole moment always prove to be zero.

The generalisation of the obtained results to the case of a spheroid with internal losses leads to a much more complicated problem than in the spherical case. The matter is that because a general analytic solution of the problem on the dipole emission is absent in the case of a spheroid, the perturbation theory over the wave vector $\boldsymbol{k}$ can be used [60]. If only the main terms are retained, then the rate of radiative losses for the atom located on the pole will be described by the expression

$$\frac{\gamma^{\text{radiative}}_{\xi,\eta=1}}{\gamma_0} = \left|1 + G_{10}\frac{\mathrm{d}}{\mathrm{d}\xi}Q_1(\xi)\right|^2 + \mathrm{O}(k^2f^2), \tag{5.36}$$

whereas the losses inside the spheroid will be described by the expression

$$\frac{\gamma^{\text{losses}}_{\xi,\eta=1}}{\gamma_0} = \frac{\gamma^{\text{total}}_{\xi,\eta=1}}{\gamma_0} - \frac{\gamma^{\text{radiative}}_{\xi,\eta=1}}{\gamma_0} = -2\left(\mathrm{Im}G_{10}\frac{\mathrm{d}}{\mathrm{d}\xi}Q_1(\xi)\right)^2 \tag{5.37}$$

$$-\frac{3}{2(k_0f)^3}\,\mathrm{Im}\sum_{n=1}^{\infty}(2n+1)\left[G_{n0}\left(\frac{\mathrm{d}}{\mathrm{d}\xi}Q_n(\xi)\right)^2 + \mathrm{O}(k^2f^2)\right].$$

Expressions (5.36) and (5.37) are consistent in the limit $\xi, \xi_0 \to \infty$ with expressions (3.21) and (3.22) found for a spherical particle. The losses inside a spheroidal particle vanish when the dielectric constant is real. If $\varepsilon'' \neq 0$, then losses (5.37) inside the spheroidal particle can exceed the radiative losses (5.36).

As for a dielectric microsphere, the conditions can be found for spheroids at which the solution of the static problem does not exist and the field inside the spheroid can strongly increase (electrodynamic trap, plasmon resonance). However, in spheroids, unlike a sphere, the dielectric constant at which an electrodynamic trap appears, depends both on the dipole orientation and the spheroid shape. The dependence of the critical dielectric constant, at which the trap appears, on the axial ratio of the ellipsoid is readily obtained from expressions (5.30)–(5.34) and is shown in Fig. 13. One can see that when the dipole is oriented parallel to the spheroid axis, the critical dielectric constant changed from $-\infty$ to -2, whereas it varies from -2 to -1 for all other orientations.

Fig. 14 shows the dependences of the decay rates on the ellipsoid axial ratio for dipoles oriented parallel to the axis of gold ($\varepsilon = -8.37 + i1.16$, $\lambda = 600$ nm) and silver ($\varepsilon = -15.37 + i0.231$, $\lambda = 632.8$ nm) spheroids. One can see that the spontaneous decay rate strongly increases (by a factor of $10^4 - 10^6$) for the Ag spheroid with $b/a \approx 0.2$ and the Au spheroid with $b/a \approx 0.35$. These results are consistent, at least qualitatively, with the experimental results of paper [50].

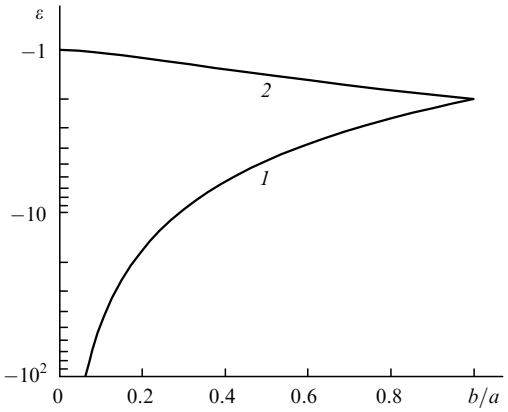

Figure 13. Critical dielectric constant, at which an electrodynamic trap (plasmon resonance) appears, as a function of the spheroid axial ratio b/a for a dipole oriented parallel to the spheroid axis (*1*) and for other dipole orientations (*2*).

As a whole, the effect of a spheroid on spontaneous emission of an atom is intermediate between the effects of a sphere and a cylinder and makes it possible to control efficiently the rates of radiative and nonradiative decay of excited states of atoms. An important specific feature of a spheroid is that, by varying its shape, i. e., its axial ratio, the spheroid can be tuned to plasmon resonances of a substance. On the one hand, this allows one to control spontaneous decay processes, and on the other, to measure the frequencies of plasmon oscillations in the spheroid.

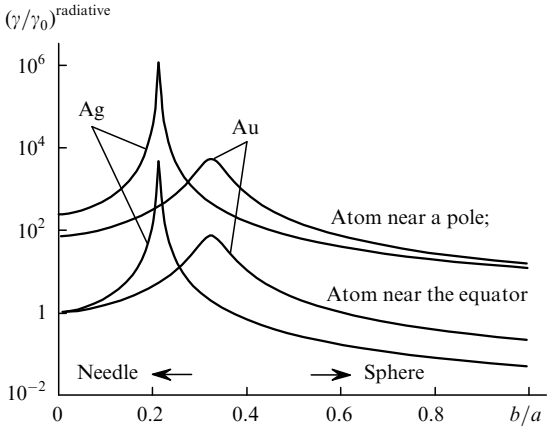

Figure 14. Spontaneous decay rates in an atom located near gold ($\varepsilon = -8.37 + i1.16$, $\lambda = 600$ nm [92]) and silver ($\varepsilon = -15.37 + i0.231$, $\lambda = 632.8$ m [93]) as functions of the spheroid axial ratio b/a for the dipole oriented parallel to the spheroid axis.

6. Spontaneous emission of an atom located near a perfectly conducting conical surface

The problem of simulating spontaneous emission of an atom located near a spike (the tip of a scanning microscope, Fig. 1) is possibly the most important and most complicated of the problems considered in our review. To solve this problem, special numerical methods have been developed which allowed the calculation of the spontaneous decay rates near a dielectric pyramidal spike [109]. Unfortunately, these methods proved to be too complicated for making any conclusions about the physics of the processes involved. For this reason, the study of model problems and, in particular, the emission of an atom located near a perfectly conducting conical surface becomes very important.

The geometry of this problem is shown in Fig. 15. The classical solution of the axially symmetrical problem on the dipole emission near a cone was found in papers [102, 110]:

$$E_r = \frac{\partial^2 U}{\partial r^2} + k^2 U,\ E_\theta = \frac{1}{r}\frac{\partial^2 U}{\partial r \partial \theta},\ E_\varphi = \frac{1}{r\sin\theta}\frac{\partial^2 U}{\partial r \partial \varphi},$$

$$U = 2id_0 k \frac{r}{r_0}\sum_{n=1}^{\infty} P_{\nu_n}(\cos\theta)\frac{j_{\nu_n}(kr_0)h_{\nu_n}^{(1)}(kr)}{N_n}. \tag{6.1}$$

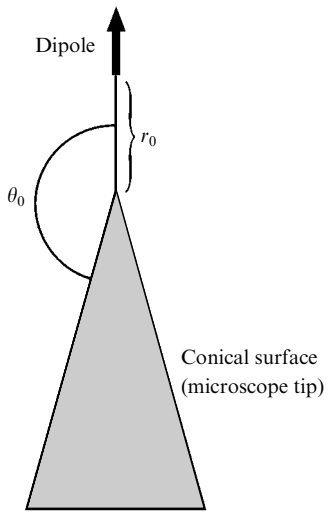

Figure 15. Geometry of a conical case.

Here, d_0 is the oscillation amplitude of the dipole moment; P_ν, j_ν, and $h_\nu^{(1)}$ are the Legendre functions and spherical Bessel and Hankel functions, respectively [107]; ν_n is the set of solutions of the equation $P_{\nu_n}(\cos\theta_0) = 0$, which provide the fulfilment of the boundary conditions on the cone surface; and

$$N_n = \int_0^{\theta_0} \sin\theta \mathrm{d}\theta P_{\nu_n}^2(\cos\theta)$$

$$= -\frac{\nu_n}{2\nu_n + 1} P_{\nu_n - 1}(\cos\theta_0)\frac{\partial P_{\nu_n}(\cos\theta_0)}{\partial \nu_n} \tag{6.2}$$

is the norm.

For not very small apex angles ($\pi/6 < \theta_0 < 5\pi/6$), we can estimate roots and norms by using approximate expressions

$$v_n = \frac{\pi}{\theta_0}\left(n - \frac{1}{4}\right) - \frac{1}{2} + \frac{\cot\theta_0}{8\pi n} + \mathrm{O}\left(\frac{1}{n^2}\right) \quad n = 1, 2, 3, \ldots,$$

$$N_n = \frac{1}{2v_n + 1}\left(\frac{3}{2} + \frac{1}{\pi}\right)\left[\frac{\Gamma(v_n + 1)}{\Gamma(v_n + 3/2)}\right]^2, \tag{6.3}$$

where Γ is gamma function. To calculate the spontaneous decay rate, we calculate the emitted energy flux in the wave zone and divide it by the energy flux from an oscillator in a free space. As a result, we obtain for the relative transition rate [111]

$$\frac{\gamma}{\gamma_0} = \frac{3}{(kr_0)^2}\sum_n \frac{v_n(v_n + 1)}{N_n} j_{v_n}^2(kr_0). \tag{6.4}$$

For $\theta_0 = \pi/2$, a conical surface becomes planar and the expression for the transition rate is simplified:

$$\frac{\gamma}{\gamma_0} = 1 - \frac{3\cos(2kr_0)}{(2kr_0)^2} + \frac{3\sin(2kr_0)}{(2kr_0)^3}, \tag{6.5}$$

coinciding, of course, with the expression for the transition rate in the presence of a conducting plane [16].

In the region of small distances from the cone apex $kr_0 \ll 1$, the first term in (6.4) plays a dominant role, and we have

$$\frac{\gamma}{\gamma_0} \approx \frac{3\pi}{16}\frac{v_1(v_1 + 1)}{N_1\Gamma^2(v_1 + 3/2)}\left(\frac{kr_0}{2}\right)^{2v_1 - 2}, \tag{6.6}$$

Using the approximate expression (6.3) for the norm, we obtain

$$\frac{\gamma}{\gamma_0} \approx \frac{3\pi^2}{8(3\pi + 2)}\frac{v_1(v_1 + 1)(2v_1 + 1)}{\Gamma^2(v_1 + 1)}\left(\frac{kr_0}{2}\right)^{2(v_1 - 1)},$$

$$v_1 = \frac{3\pi}{4\theta_0} - \frac{1}{2} + \frac{\cot\theta_0}{8\pi}. \tag{6.7}$$

When the distance from the atom to the spike is not small, the numerical summation should be performed in Eqn (6.4). The results of the calculations are presented in Fig. 16. One can see from this figure that a conical spike ($\theta_0 > \pi/2$) strongly affects the transition rates (increasing them) only when the atom approaches the spike apex. As the opening angle decreases ($\theta_0 \to \pi$), the influence of the spike is manifested at decreasing distances of the atom from the angle apex. This means that an infinitely sharp needle does not affect in fact the spontaneous emission of the atom located at any small (but finite) distance from its end.

A more interesting behaviour is observed when an atom is located inside a conical spike [inside a microscope tip ($\theta_0 < \pi/2$)]. In this case, interference effects appear and the transition rate becomes substantially dependent on the parameters of the problem. The rate strongly increases at some points and strongly decreases at other points. As the atom approaches the spike apex, the transition rate tends to zero because emission cannot escape at all from such a region.

The case of a perfectly conducting surface considered above is only the first step in the study of the influence of a spike on spontaneous emission of an atom. Further studies should take into account the specific properties of the substance forming the spike or the void. This may lead to the results that will substantially differ from those presented above, as was the case on passing from a perfectly conducting cylinder to a dielectric cylinder.

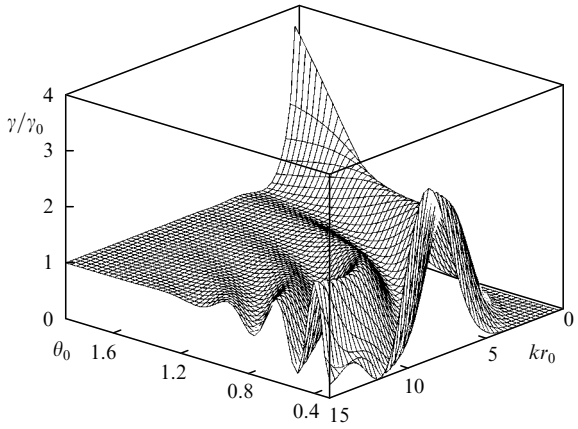

Figure 16. Rates of the dipole E_1 transitions in an atom located near a perfectly conducting conical surface as functions of the opening angle θ_0 and the distance between the atom and the cone apex for the radial orientation of the dipole moment.

7. Conclusions

We have considered the studies of spontaneous emission of an atom located near bodies of different shapes and described various quantum-mechanical and classical methods for calculating spontaneous emission rates in the presence of nanobodies. The theoretical results well agree with the experimental data for an emitting atom located near a planar interface [36, 37].

A great part of the review was devoted to particular calculations of the emission of an atom located near spherical, cylindrical, spheroidal, and conical bodies. A special attention was paid to nanobodies, i.e., the bodies in which at least one of the characteristic sizes was small compared to the emission wavelength. In addition, we focused attention on the atom located near the body surface. In all these cases, we obtained simple analytic expressions for the decay rates with characteristic values of the parameters. The asymptotic expressions were presented for the transition rates in the case of the applicability of the perturbation theory over the wave vector [60]. It was shown that the radiative and nonradiative dipole transition rates could increase by several orders of magnitude in the presence of nanobodies, in qualitative agreement with the experimental data.

The results presented in the review can be used in various fields of nanophysics, in particular, for describing apertureless scanning microscopes. In addition, nanobodies can be used for studying the properties of weak dipole and quadrupole transitions, which are strongly accelerated near nanobodies [56, 57].

We also have considered spontaneous emission of an atom in the presence of nanobodies with the dielectric constant that is typical for usual dielectrics and metals. However, at present a variety of media were fabricated that possess unusual dielectric constants. In this connection, it would be interesting to consider spontaneous emission of an atom located near active media [112], near dielectric photonic crystals [29–35, 113] and, finally, near media with negative refractive indices ($\varepsilon < 0$, $\mu < 0$) [114–117], where

many new effects can be expected. Nanobodies made of materials with the negative refractive index are especially interesting because they can exhibit (unlike usual nanobodies) surface resonance modes, which substantially affect spontaneous emission [118].

Acknowledgements. The authors thank the Russian Foundation for Basic Research (V V Klimov, V S Letokhov), the Integration Program (V V Klimov, M Ducloy), and the French National Research Centre (V V Klimov, M Ducloy) for financial support of this work.

References

1. Einstein A *Mitt. Phys. Ges. (Zurich)* **18** 47 (1916); Einstein A *Sobranie Nauchnykh Trudov* (Collection of Scientific Papers) (Moscow: Nauka, 1966) vol. 3, pp. 393 – 406
2. Dirac P A M *The Principles of Quantum Mechanics* (Oxford, 1958; Moscow: Fizmatgiz, 1960)
3. Fermi E *Rev. Mod. Phys.* **4** 87 (1932)
4. Basov N G, Prokhorov A M *Dokl. Akad. Nauk SSSR* **101** 47 (1955); *Zh. Eksp. Teor. Fiz.* **27** 432 (1954)
5. Gordon J P , Zeiger H J, Townes C H *Phys. Rev.* **95** 282 (1954)
6. Prokhorov A M *Zh. Eksp. Teor. Fiz.* **34** 1658 (1958)
7. Schawlow A L, Townes C H *Phys. Rev.* **112** 1940 (1958)
8. Alferov Zh I *Nobel Lecture* (2000)
9. Purcell E M *Phys. Rev.* **69** 681 (1946)
10. Bunkin F V, Oraevskii A N *Izv. Vyssh. Uchebn. Zaved. Ser Radiofiz.* **2** (2) 181 (1959)
11. Kleppner D *Phys. Rev. Lett* **47** 233 (1981)
12. Goy P, Raymond J M, Gross M, Haroche S *Phys. Rev. Lett.* **50** 1903 (1983)
13. Hulet R G, Hilfer E S, Kleppner D *Phys. Rev. Lett.* **55** 2137 (1985)
14. Gabrielse G, Dehmelt H *Phys. Rev. Lett.* **55** 67 (1985)
15. Berman P (Ed.) *Cavity Quantum Electrodynamics* (New York: Academic, 1994)
16. Haroche S, in *Fundamental System in Quantum Optics.* J.Dalibard, J.M.Raimond, J.Zinn-Justin (Eds) (Les Houches, 1990; Elsevier Science Publishers B V, 1992)
17. Jhe W, Anderson A, Hinds E A, Meshede D, Moi L, Haroche S *Phys. Rev. Lett.* **58** 666 (1987)
18. Braginskii V B, Il'chenko V S *Dokl. Akad. Nauk SSSR* **293** 1358 (1987)
19. Braginsky V B, Gorodetsky M L, Ilchenko V S *Phys. Lett. A* **137** 393 (1989)
20. Collot L, Lefevre-Seguine V, Brune M, Raimond J M, Haroche S *Europhys. Lett.* **23** 327 (1993)
21. Sandoghdar V, Treussart F, Hare J, Lefevre-Seguin V, Raimond J-M, Haroche S *Phys. Rev. A* **54** R1777 (1996)
22. Oraevskii A N, Skully M, Velichanskii V L *Kvantovaya Elektron.* **25** 211 (1998) [*Quantum Electron.* **28** 203 (1998)]
23. Lin H-B, Eversole J D, Merritt C D, Campillo A J *Phys. Rev. A* **45** 6756 (1992)
24. Yokoyama H, Ujihara K (Eds) *Spontaneous Emission and Laser Oscillations in Microcavities* (Boca Raton, CRC Press, 1995)
25. Choquette K, Hon H *Proc. IEEE* **85** 1730 (2000)
26. Tessler N, Denton G, Friend R *Nature* **382** 695 (1996)
27. Zhang J, Chu D, Wu S, Ho S, Bi W, Tu C, Tiberio R *Phys. Rev. Lett.* **75** 2678 (1995)
28. Slusher R E, Weisbuch C *Solid State Comm.* **92** 149 (1994)
29. Bykov V P *Zh. Eksp. Teor. Fiz.* **62** 505 (1972)
30. Bykov V P *Kvantovaya Elektron.* **1** 1557 (1974) [*Sov. J. Quantum Electron.* **4** 861 (1974)]
31. Yablonovich E *Phys. Rev. Lett.* **58** 2059 (1987)
32. John S *Phys. Rev. Lett.* **58** 2486 (1987)
33. Bykov V P *Izluchenie Atomov Vblizi Material'nykh Tel* (Emission of Atoms Near Material Bodies) (Moscow: Nauka, 1986)
34. Kurizkii G, Hans J *J. Mod. Opt.* **71** 171 (1994)
35. Joannopoulos J, Meadle R, Winn J *Photonic Crystals* (Princeton, Princeton Univ. Press, 1995)
36. Amos R, Barnes W L *Phys. Rev. B* **55** 7249 (1997)
37. Drexhage K H, in *Progress in Optics XII* (Amsterdam, North-Holland, 1974), vol. 12, p. 165
38. Pohl D W, Courjon D (Eds) *Near Field Optics* (Dordrecht, Kluwer Acad. Publ., 1992)
39. Ohtsu M (Ed) *Near Field Nanoatom Optics and Technology* (Berlin, Springer, 1998)
40. Girard C, Joachim C, Gauthier S *Rep. Prog. Phys.* **65** 893 (2000)
41. Zenhausen F, O'Boyle M, Wickramasinghe H *Appl. Phys. Lett.* **65** 1623 (1994)
42. Zenhausen F, Martin Y, Wickramasinghe H *Science* **269** 1083 (1995)
43. Bachelot R, Gleyzes P, Boccara A *Appl. Opt.* **36** 2160 (1997)
44. Hamann H F, Gallagher A, Nesbitt D J *Appl. Phys. Lett.* **76** 1953 (2000)
45. Lewis A, Liberman K *Nature* **214** 214 (1991)
46. Sekatskii S, Letokhov V S *Appl. Phys. B* **63** 525 (1996)
47. Henkel C, Sandoghdar V *Opt. Commun.* **158** 250 (1998)
48. Stöckle R M, Suh Y D, Deckert V, Zenobi R *Chem. Phys. Lett.* **318** 131 (2000)
49. Anderson M S *Appl. Phys. Lett.* **76** 3130 (2000)
50. Mohamed M B, Volkov V, Link S, El-Sayed M A *Chem. Phys. Lett.* **317** 517 (2000)
51. Oldenburg S J, Averitt R D, Westcott S L, Halas N J *Chem. Phys. Lett.* **288** 243 (1998)
52. Lyon W A, Nie S M *Anal. Chem.* **69** 3400 (1997)
53. Zander C, Drexhage K H, Han K T, Wolfrum J, Sauer M *Chem. Phys. Lett.* **286** 457 (1998)
54. Denschlag J, Umshaus G, Schmiedmayer J *Phys. Rev. Lett.* **81** 737 (1998)
55. Denschlag J, Cassetari D, Chenet A, Schneider S, Schmiedmayer J *Appl. Phys. B* **69** 291 (1999)
56. Klimov V V, Letokhov V S *Phys. Rev. A* **54** 4408 (1996)
57. Klimov V V, Ducloy M *Phys. Rev. A* **62** 043818 (2000)
58. Ducloy M, in *Nanoscale Science and Technology* (Kluber, the Netherlands, 1998) p. 235; Boustimi M, de Lesegno B V, Baundon J, Rjbert J, Ducloy M *Phys. Rev. Lett* **86** 2766 (2001)
59. Chance R R, Prock A, Sylbey R *Adv. Chem. Phys.* **37** 1 (1978)
60. Stevenson A F *J. Appl. Phys.* **24** 1134 (1953)
61. Glauber R J, Lewenstein M *Phys. Rev. A* **43** 467 (1991)
62. Wylie J M, Sipe J E *Phys. Rev. A* **30** 1185 (1984); **32** 2030 (1985)
63. Dung H T, Knoll L, Welsch D-G *Phys. Rev. A* **6205** 3804 (2000)
64. Knoll L, Scheel S, Welsch D-G *Quant-ph*/000621-27 June, 2000
65. Yeung M S, Gustafson T K *Phys. Rev. A* **54** 5227 (1996)
66. Sullivan K G, Hall D G *J. Opt. Soc. Am. A* **14** 1150 (1970)
67. Wu B S T, Eberlein C *Proc. R. Soc. Lond. A* **455** 2487 (1999)
68. Gersen H, García-Parajó M F, Novotny L , Veerman J A, Kuipers L , van Hulst N F *Phys. Rev. Lett* **85** 5312 (2000)
69. Markov G T *Zh. Tekh. Fiz.* **23** 838 (1953)
70. Barut A O, Dowling J P *Phys. Rev. A* **36** 649 (1987)
71. Ruppin R *J. Chem. Phys.* **76** 1681 (1982)
72. Chew H, McNulty P J, Kerker M *Phys. Rev. A* **13** 396 (1976)
73. Chew H *J. Chem. Phys.* **87** 1355 (1987)
74. Chew H *Phys. Rev. A* **38** 3410 (1988)
75. Jhe W, Kim J W *Phys. Rev. A* **51** 1150 (1995)
76. Jhe W, Kim JW *Phys. Lett. A* **197** 192 (1995)
77. Jhe W, Jang K *Phys. Rev. A* **53** 1126 (1995)
78. Dutta G S, Agarwal G S *Opt. Commun.* **115** 597 (1995)
79. Agarwal G S *J. Mod. Opt.* **45** 449 (1998)
80. Klimov V V, Ducloy M, Letokhov V S *J. Mod. Opt.* **43** 549 (1996)
81. Klimov V V, Ducloy M, Letokhov V S *J. Mod. Opt.* **43** 2251 (1996)
82. Klimov V V, Ducloy M, Letokhov V S *Phys. Rev. A* **59** 2996 (1999)
83. Davydov A S *Kvantovaya Mechanika* (Quantum Mechanics) (Moscow: Nauka, 1973)
84. Ching S C, Lai H M, Young K J *Opt. Soc. Am. B* **4** 1995 (1987)
85. Ching S C, Lai H M, Young K J *Opt. Soc. Am. B* **4** 2004 (1987)
86. Jackson J.D. *Classical Electrodynamics* (New York: Wiley, 1975)
87. Stratton J A *Teoriya Electromagnetizma* (The Theory of Electromagnetism) (Moscow: GITTL, 1948)

88. Born M, Wolf E *Principles of Optics* (Oxford: Pergamon Press, 1969; Moscow: Nauka, 1973)
89. Mie G *Ann. Physik IV* **25** 377 (1908)
90. Belkina M G, Vainshtein L A, in *Diffraktsiya Elektromagnitnykh Voln na Nekotorykh Telakh Vrashcheniya* (Diffraction of Electromagnetic Waves by Some Bodies of Revolution) (Moscow: Sov. Radio, 1957) p. 57
91. Courant R, Hilbert D *Methods of Mathematical Physics* (New York: Wiley-InterScience, 1962), vol. 1
92. Hass G, Hadley L, in *American Institute of Physics Handbook* (New York: McGraw-Hill, 1963) p. 6
93. Shu Q Q, Hansma P K *Thin Solid Films* (to be published)
94. Vaganov R B, Katsenelenbaum B Z *Osnovy Teorii Diffraktsii* (Fundamentals of the Diffraction Theory) (Moscow: Nauka, 1982)
95. Markov G T, Chaplin A F V*ozbuzhdenie Elektromagnitnykh Voln* (Excitation of Electromagnetic Waves) (Moscow: Radio i Svyaz', 1983)
96. Katsenelenbaum B Z *Zh. Tekh. Fiz.* **19** 1182 (1949)
97. Nha H, Jhe W *Phys. Rev. A* **56** 2213 1(997)
98. Enderlein J *Chem. Phys. Lett.* **301** 430 (1999)
99. Zakowicz W, Janowicz M *Phys. Rev. A* **62** 013820 (2000)
100. DeBroglie L *Problemes de Propagation Guidees des Ondes Electromagnetiques* (Paris, 1941)
101. Klimov V V, Ducloy M *Opt. Commun.* (to be published)
102. Vainshtein L A *Elektromagnitnye Volny* (Electromagnetic Waves) (Moscow: Radio I Svyaz', 1988)
103. Farafonov V G *Diff. Uravn.* **19** 1765 (1983)
104. Asano S, Yamamoto G *Appl. Opt.* **14** 29 (1975)
105. Belkina M G, in *Diffraktsiya Elektromagnitnykh Voln na Nekotorykh Telakh Vrashcheniya* (Diffraction of Electromagnetic Waves by Some Bodies of Revolution) (Moscow: Sov. Radio, 1957) p. 126
106. Smite V *Electrostatics and Electrodynamics* (Moscow: Inostrannaya Literatura, 1954)
107. Abramowitz M, Stegun I A (Eds) *Handbook of Mathematical Functions* (Washington; NBS, 1964; Moscow: Nauka, 1979)
108. Klimov V V, Ducloy M, Letokhov V S *European Phys. J.* (to be published)
109. Girard C, Dereux A *Rep. Prog. Phys.* **59** 657 (1996)
110. Macdonald H M *Electric Waves* (Cambridge, Cambridge University Press, 1902)
111. Klimov V V *Pis'ma Zh Eksp. Teor. Fiz.* **68** 610 (1998)
112. Kocharovsky V V, Kocharovsky Vl V, Belyanin A A *Phys. Rev. Lett.* **76** 3285 (1996)
113. Kamli A, Babiker M *Phys. Rev. A* **62** 043804 (2000)
114. Veselago V G *Usp. Fiz. Nauk* **10** 509 (1968)
115. Smith D R, Padilla W J, Vier D C, Nemat-Nesser S C, Schultz S *Phys. Rev. Lett.* **84** 4184 (2000)
116. Smith D R, Kroll N *Phys. Rev. Lett.* **85** 2933 (2000)
117. Fitzgerald R *Physics Today* (5) 17 (2000)
118. Klimov V V *Quant-ph*/0102081-10 March 2001